Electronic Supplementary Material (ESI) for Physical Chemistry Chemical Physics.

Unravelling ionic liquid solvent effects for a non-polar Cope rearrangement reaction.

*Gavin J. Smith, Spyridon Koutsoukos, Ben Lancaster, Julian Becker, Tom Welton and Patricia A. Hunt**

Section 1. Synthesis

Section 2: Structure Generation, CREST Data and B3LYP Data Reactions A and B

Section 3. TS Conformers

Section 4. Reaction Energies

Section 5: Solvation Energies

Section 6: Structure Generation, CREST Data and B3LYP Data Reactions Reaction C

Section 7: AIMALL and Jmol Volume Data

Section 8: Structures for TS-solvent cluster analysis

Section 9: Association Energy of TS-solvent clusters

Section 10: AIM Analysis of TS-solvent clusters

Section 11: NCI plots of TS-solvent clusters

Section 12: NBO and CHelpG Charge Analysis

Section 13: Density Difference of TS-solvent clusters

Section 14: Comparing GP and SMD electrostatic polarisation

Section 15: Computed Alpha

Section 16: HPLC Data

Section 17: NMR of Relevant Compounds

Section 1. Synthesis

Synthesis and Characterisation of ILs

$[C_4C_1im][NTf_2]$, $[C_4C_1C_1im][NTf_2]$, $[C_4C_1pyrr][NTf_2]$ were synthesised from their bromide or chloride precursors via salt metathesis. $[C_4C_1im][OTf]$ was available from lab stock and was characterised before use. The halide precursors $[C_4C_1im]Cl$, $[C_4C_1C_1im]Br$, $[C_4C_1pyrr]Br$ were used from stock in the lab and characterised before use.

Characterisation of halide IL-precursors

1-Butyl-1-methylpyrrolidinium bromide $[C_4C_1pyrr]Br$

^1H NMR (400 MHz, DMSO) δ 3.51 – 3.37 (m, 4H, **Pyrr** CH_2-**CH_2**-N-**CH_2**-CH_2), 3.35 – 3.24 (m, 2H, N-**CH_2**-CH_2-CH_2-CH_3), 2.97 (s, 3H, N-**CH_3**), 2.07 (s, 4H, **Pyrr CH_2**-CH_2-N-CH_2-**CH_2**), 1.67 (m, 2H, N-CH_2-**CH_2**-CH_2-CH_3), 1.31 (m, 2H, N-CH_2-CH_2-**CH_2**-CH_3), 0.97 – 0.89 (m, 3H, N-CH_2-CH_2-CH_2-**CH_3**).
$^{13}C\{^1H\}$ NMR (101 MHz, DMSO) δ 63.35 (**Pyrr** CH_2-**CH_2**-N-**CH_2**-CH_2), 62.78 (N-**CH_2**-CH_2-CH_2-CH_3), 47.45 (N-**CH_3**), 24.93 (N-CH_2-**CH_2**-CH_2-CH_3), 21.05 (**Pyrr CH_2**-CH_2-N-CH_2-**CH_2**), 19.31 (N-CH_2-CH_2-**CH_2**-CH_3), 13.52 (N-CH_2-CH_2-CH_2-**CH_3**).

MS (ES): +ve ion m/z calculated (142.27) found (142.15), -ve ion m/z calculated (79.90) found (78.75)

1-Butyl-2,3-dimethylimidazolium bromide $[C_4C_1C_1im]Br$

^1H NMR (400 MHz, DMSO) δ 7.67 (d, J = 2.1 Hz, 1H, im-N-**CH**-CH-N), 7.64 (d, J = 2.1 Hz, 1H, im-N-CH-**CH**-N), 4.11 (t, J = 7.3 Hz, 2H, N-**CH_2**-CH_2-CH_2-CH_3), 3.75 (s, 3H, N-**CH_3**), 2.58 (s, 3H, im-**CH_3**), 1.74 – 1.58 (m, 2H, N-CH_2-**CH_2**-CH_2-CH_3), 1.27 (dt, J = 14.7, 7.4 Hz, 2H, N-CH_2-CH_2-**CH_2**-CH_3), 0.90 (t, J = 7.4 Hz, 3H, N-CH_2-CH_2-CH_2-**CH_3**).
$^{13}C\{^1H\}$ NMR (101 MHz, DMSO) δ 144.21 (im-N-**C**(CH_3)-N), 122.29 (im-N-**CH**-CH-N), 120.86 (im-N-CH-**CH**-N), 47.26 (N-**CH_2**-CH_2-CH_2-CH_3), 34.68 (N-**CH_3**), 31.17, (im-N-C(**CH_3**)-N), 18.86 (N-CH_2-**CH_2**-CH_2-CH_3), (13.39 N-CH_2-CH_2-**CH_2**-CH_3), 9.18 (N-CH_2-CH_2-CH_2-**CH_3**).

MS (ES): +ve m/z calculated (153.25) found (153.1), -ve m/z calculated (79.90) found (78.9, 80.9)

1-Butyl-3-methylimidazolium chloride $[C_4C_1im]Cl$

^1H NMR (400 MHz, CDCl3) δ 10.46 (s, 1H, im-N-**CH**-N), 7.61 (d, J = 1.9 Hz, 1H, im-N-**CH**-CH-N), 7.44 (d, J = 1.9 Hz, 1H, im-N-CH-**CH**-N), 4.23 (t, J = 7.4 Hz, 2H, N-**CH_2**-CH_2-CH_2-CH_3), 4.02 (s, 3H N-**CH_3**), 1.80 (m, 2H, N-CH_2-**CH_2**-CH_2-CH_3), 1.27 (m, 2H, N-CH_2-CH_2-**CH_2**-CH_3), 0.85 (t, J = 7.3 Hz, 3H, N-CH_2-CH_2-CH_2-**CH_3**).
$^{13}C\{^1H\}$ NMR (101 MHz, CDCl3) δ 137.72 (im-N-**CH**-N), 123.68 (im-N-**CH**-CH-N), 121.98(im-N-CH-**CH**-N), 49.67 (N-**CH_2**-CH_2-CH_2-CH_3), 36.46 (N-**CH_3**), 32.09 (N-CH_2-**CH_2**-CH_2-CH_3), 19.37 (13.39 N-CH_2-CH_2-**CH_2**-CH_3), 13.36 (N-CH_2-CH_2-CH_2-**CH_3**).

MS (ES): +ve m/z calculated (139.12) found (139.11)

Synthesis and Characterisation of the ILs

1-Butyl-3-methylimidazolium bis(trifluoromethylsulfonyl)imide $[C_4C_1im][NTf_2]$

$[C_4C_1im]Cl$ (12.49g, 71.5 mmol, 1eq) was dissolved in CH_2Cl_2 (50ml). $LiNTf_2$ (24.6g, 85.2 mmol 1.10eq) was dissolved in water (80ml). Under stirring the solution of $LiNTf_2$ was slowly added to the solution of $[C_4C_1im]Cl$. The reaction was stirred overnight. The reaction mixture was extracted with water until halide free (tested with aq. $AgNO_3$). The organic phase was dried over $MgSO_4$, filtered and evaporated to yield the product as a clear colourless liquid (27.7g, 65.8mmol, 92.0%).

^{1}H NMR (400 MHz, DMSO) δ 9.10 (d, J = 1.7 Hz, 1H, im-N-**CH**-N), 7.76 (t, J = 1.8 Hz, 1H im-N-CH-**CH**-N), 7.69 t, J = 1.7 Hz, 1H, im-N-CH-**CH**-N), 4.15 (t, J = 7.2 Hz, 2H, N-**CH$_2$**-CH$_2$-CH$_2$-CH$_3$), 3.84 (s, 3H), 1.84 – 1.69 (m, 2H, N-CH$_2$-**CH$_2$**-CH$_2$-CH$_3$), 1.26 (dq, J = 7.4 Hz, 2H, N-CH$_2$-CH$_2$-**CH$_2$**-CH$_3$), 0.90 (t, J = 7.4 Hz, 3H, N-CH$_2$-CH$_2$-CH$_2$-**CH$_3$**).
^{13}C{^{1}H} NMR (101 MHz, DMSO) δ 136.51 (im-N-**CH**-N), 123.63 (im-N-**CH**-CH-N), 122.27 (im-N-**CH**-CH-N), 119.49 (d, J = 321.8 Hz,), 48.50 (N-**CH$_2$**-CH$_2$-CH$_2$-CH$_3$), 35.74 (N-**CH$_3$**), 31.35 (N-CH$_2$-**CH$_2$**-CH$_2$-CH$_3$), 18.77 (N-CH$_2$-CH$_2$-**CH$_2$**-CH$_3$), 13.24 (N-CH$_2$-CH$_2$-CH$_2$-**CH$_3$**).
^{19}F NMR (377 MHz, DMSO) δ -78.75 (**CF$_3$**-SO$_2$-N$^-$-SO$_2$-**CF$_3$**).

MS (ES): +ve m/z calculated (139.22) found (139.12), -ve m/z calculated (280.14) found (279.92)

<u>1-Butyl-2,3-dimethylimidazolium bis(trifluoromethylsulfonyl)imide [C$_4$C$_1$C$_1$im][NTf$_2$]</u>
[C$_4$C$_1$C$_1$im]Br (2.15g, 9.22mmol, 1eq) was dissolved in CH$_2$Cl$_2$ (7ml). LiNTf$_2$ (2.91g, 10.14mmol 1.10eq) was dissolved in water (12ml). Under stirring the solution of LiNTf$_2$ was slowly added to the solution of [C$_4$C$_1$C$_1$im]Br. The reaction was stirred overnight. The reaction mixture was extracted with water until halide free (tested with aq. AgNO$_3$). The organic phase was dried over MgSO$_4$, filtered and evaporated to yield the product as a clear colourless liquid (2.70g, 6.40mmol, 69.9%)

^{1}H NMR (400 MHz, DMSO) δ 7.64 (d, J = 2.1 Hz, 1H, im-N-**CH-**CH-N), 7.61 (d, J = 2.1 Hz, 1H, im-N-CH-**CH-**N), 4.10 (t, J = 7.3 Hz, 2H, N-**CH$_2$**-CH$_2$-CH$_2$-CH$_3$), 3.74 (s, 3H, N-**CH$_3$**), 2.57 (s, 3H, im-**CH$_3$**), 1.74 – 1.62 (m, 2H, N-CH$_2$-**CH$_2$**-CH$_2$-CH$_3$), 1.28 (dq, J = 14.8, 7.4 Hz, 2H, N-CH$_2$-CH$_2$-**CH$_2$**-CH$_3$), 0.90 (t, J = 7.4 Hz, 3H, N-CH$_2$-CH$_2$-CH$_2$-**CH$_3$**).
^{13}C NMR{^{1}H} (101 MHz, DMSO) δ 144.21 (im-N-**C**(CH$_3$)-N), 122.29 (im-N-**CH**-CH-N), 120.86 (im-N-CH-**CH**-N), 119.48 (q, 323.2 Hz (**C**F$_3$-SO$_2$-N$^-$-SO$_2$-**C**F$_3$)) 47.26 (N-**CH$_2$**-CH$_2$-CH$_2$-CH$_3$), 34.68 (N-**CH$_3$**), 31.17, (im-N-C(**CH$_3$**)-N), 18.86 (N-CH$_2$-**CH$_2$**-CH$_2$-CH$_3$), 13.39 (N-CH$_2$-CH$_2$-**CH$_2$**-CH$_3$), 9.18 (N-CH$_2$-CH$_2$-CH$_2$-**CH$_3$**).
^{19}F NMR (377 MHz, DMSO) δ -78.73 (**CF$_3$**-SO$_2$-N$^-$-SO$_2$-**CF$_3$**).

MS (ES): +ve m/z calculated (153.25) found (153.13), -ve m/z calculated (280.14) found (279.23)

<u>1-Butyl-1-methylpyrrolidinium bis(trifluoromethylsulfonyl)imide [C$_4$C$_1$pyrr][NTf$_2$]</u>
[C$_4$C$_1$pyrr]Br (6.00g, 27.01mmol, 1eq) was dissolved in CH$_2$Cl$_2$ (20ml). LiNTf$_2$ (8.53g, 29.71mmol 1.10eq) was dissolved in water (30ml). Under stirring the solution of LiNTf$_2$ was slowly added to the solution of [C$_4$C$_1$pyrr]Br. The reaction was stirred overnight. The reaction mixture was extracted with water until halide free (tested with aq. AgNO$_3$). The organic phase was dried over MgSO$_4$, filtered and evaporated to yield the product as a clear colourless liquid (8.90g, 21.22mmol, 79.5%)

^{1}H NMR (400 MHz, DMSO) δ 3.52 – 3.36 (m, 4H, **pyrr** CH$_2$-**CH$_2$**-N-**CH$_2$**-CH$_2$), 3.33 – 3.24 (m, 2H, N-**CH$_2$**-CH$_2$-CH$_2$-CH$_3$), 2.97 (s, 3H, N-**CH$_3$**), 2.15 – 2.02 (m, 4H, **pyrr CH$_2$**-CH$_2$-N-CH$_2$-**CH$_2$**), 1.67 (m, 2H, N-CH$_2$-**CH$_2$**-CH$_2$-CH$_3$), 1.32 (h, J = 7.4 Hz, 2H, N-CH$_2$-CH$_2$-**CH$_2$**-CH$_3$), 0.93 (t, J = 7.4 Hz, 3H, N-CH$_2$-CH$_2$-CH$_2$-**CH$_3$**).
^{13}C{^{1}H} NMR (101 MHz, DMSO) δ 119.50 (q, J = 321.8 Hz, **CF$_3$**-SO$_2$-N$^-$-SO$_2$-**CF$_3$**), 63.41 (**pyrr** CH$_2$-**CH$_2$**-N-**CH$_2$**-CH$_2$), 62.93 (N-**CH$_2$**-CH$_2$-CH$_2$-CH$_3$), 47.48 (N-**CH$_3$**), 24.92 (N-CH$_2$-**CH$_2$**-CH$_2$-CH$_3$), 21.06 (**pyrr CH$_2$**-CH$_2$-N-CH$_2$-**CH$_2$**), 19.30 (N-CH$_2$-CH$_2$-**CH$_2$**-CH$_3$), 13.42 (N-CH$_2$-CH$_2$-CH$_2$-**CH$_3$**).
^{19}F NMR (377 MHz, DMSO) δ -78.77 (**CF$_3$**-SO$_2$-N$^-$-SO$_2$-**CF$_3$**).

MS (ES): +ve m/z calculated (142.27) found (142.15), -ve m/z calculated (280.14) found (279.22)

<u>1-Butyl-3-methylimidazolium trifluoromethanesulfonate [C_4C_1im][OTf] (Used from stock)</u>
^{1}H NMR (400 MHz, DMSO) δ 9.09 (s, 1H, im-N-**CH**-N), 7.76 (d, J = 1.8 Hz, 1H, im-N-**CH**-CH-N), 7.69 (d, J = 2.0 Hz, 1H, im-N-CH-**CH**-N), 4.16 (t, J = 7.2 Hz, 2H, N-**CH_2**-CH_2-CH_2-CH_3), 3.84 (s, 3H), 1.76 (p, J = 7.3 Hz, 2H, N-CH_2-**CH_2**-CH_2-CH_3), 1.26 (m, 2H, N-CH_2-CH_2-**CH_2**-CH_3), 0.90 (t, J = 7.3 Hz, 3H, N-CH_2-CH_2-CH_2-**CH_3**).
^{13}C{^{1}H} NMR (101 MHz, DMSO) δ 136.49 (im-N-**CH**-N), 123.61 (im-N-**CH**-CH-N), 122.26 (im-N-CH-**CH**-N), 48.50 (N-**CH_2**-CH_2-CH_2-CH_3), 120.68 (q, J = 322.08 Hz, $^-$O-SO_2-**CF_3**), 35.73 (N-**CH_3**), 31.34 (N-CH_2-**CH_2**-CH_2-CH_3), 18.76 (13.39 N-CH_2-CH_2-**CH_2**-CH_3), 13.24 (N-CH_2-CH_2-CH_2-**CH_3**).
^{19}F NMR (377 MHz, DMSO) δ -77.82 ($^-$O-SO_2-**CF_3**).

MS (ES): +ve m/z cation calculated (139.22) found (139.12), -ve m/z anion calculated (149.06) found (148.59)

Synthesis and Characterisation of Dienes

Both the product and the starting material of reaction B are synthesised in a two-step synthesis via *tert*-butyl dicarbonate (Boc) protected cinnamyl alcohol, tert-butyl cinnamyl carbonate (figure S1.1). The final dienes are synthesised by a Suzuki coupling between *tert*-butyl cinnamyl carbonate and allylboronic acid pinacol ester.

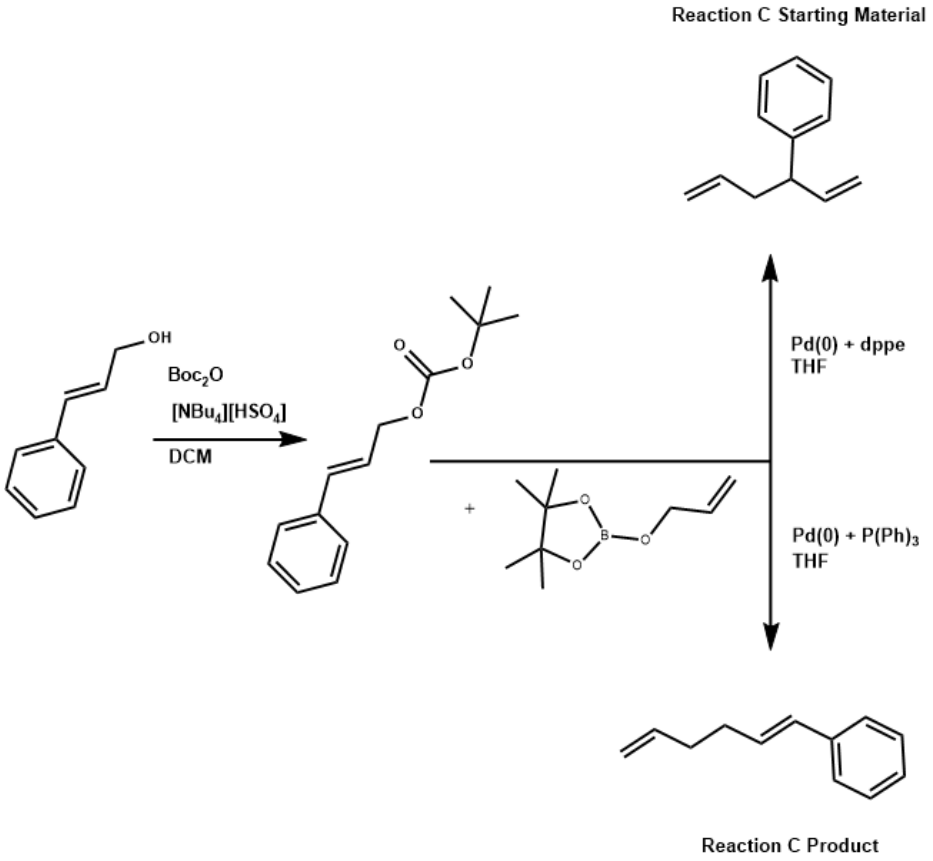

Figure S1.1: Reaction schemes to synthesise the starting material and product of reaction C from cinnamyl alcohol.

tert-Butyl cinnamyl carbonate

Tetrabutylammonium hydrogensulfate (0.1g, 0.3 mmol, 0.02eq) was dissolved in in CH_2Cl_2 (7ml). The solution was cooled to 0°C and cinnamyl alcohol (2g, 14.9 mmol, 1eq) was added and stirred until dissolved. Di-*tert*-butyldicarbonate (3.91g, 17.9 mmol, 1.2eq) was added and stirred until dissolved. At 0°C 3M aq. NaOH solution (6ml) was added dropwise over 10 min. The reaction was stirred at 0°C for 30 min. The reaction was warmed to RT and stirred overnight. The reaction is monitored by TLC (1:20 ethyl acetate:hexane) until only trace amounts of the starting material are visible. Additional portions of di-*tert*-butyldicarbonate (0.2eq) were added as required if no further product formation was observed and starting material was still present. Upon completion the reaction mixture was diluted with water and extracted with diethyl ether. The combined organic phases were washed with hydrochloric acid (1 M), water and brine. The organic layer was dried with $MgSO_4$, filtered and evaporated under reduced pressure. To remove excess di-*tert*-butyl decarbonate, the crude material was dissolved in CH_2Cl_2 and imidazole (1.01 g, 14.9 mmol, 1eq) was added. The reaction was stirred overnight. The mixture was diluted with water and washed with hydrochloric acid (1%), water and brine. The organic layer was dried with $MgSO_4$, filtered and evaporated under reduced pressure. The crude material was passed through a silica gel column (1:20 ethyl acetate:hexane) to yield the product as a colourless liquid (2.3g, 9.8 mmol, 65.8%).

^{1}H NMR (400 MHz, DMSO) δ 7.50 – 7.43 (m, 2H, 2x Ph-**H**), 7.39 – 7.31 (m, 2H, 2x Ph-**H**), 7.30 – 7.25 (m, 1H, Ph-**H**), 6.68 (dt, J = 16.0, 1.5 Hz, 1H, Ph-**CH**=CH-CH_2-OR), 6.37 (dt, J = 16.0, 6.2 Hz, 1H, Ph-CH=**CH**-CH_2-OR), 4.68 (dd, J = 6.3, 1.4 Hz, 2H, Ph-CH=CH-**CH_2**-OR), 1.43 (s, 9H, R-O-C(**CH_3**)$_3$).
^{13}C{^{1}H} NMR (101 MHz, DMSO) δ 152.81 (RO(**C**=O)OR), 135.90 (**Ph**), 133.31 (Ph-**CH**=CH-CH_2-OR), 128.70 (**Ph**), 128.09 (**Ph**), 126.55 (**Ph**), 123.49 (Ph-CH=**CH**-CH_2-OR), 81.55 R-O-**C**$(CH_3)_3$, 66.90 (Ph-CH=CH-**CH_2**-OR), 27.38 (R-O-C(**CH_3**)$_3$).

MS (ES): +ve m/z calculated (234.30) found (234.2)

3-Phenyl-1,5-hexadiene

A solution of allyl boronic acid pinacol ester (1.21 g, 7.21 mmol, 1.3eq) and *tert*-butyl cinnamyl carbonate (1.30 g, 5.55 mmol, 1eq) in dry and degassed tetrahydrofuran (12 mL) was prepared. A separate solution of tris(dibenzylideneacteone)dipalladium(0) (0.254 g, 0.277mmol, 0.05eq) and 1,2-bis(diphenylphosphino)ethane (0.192 g, 0.555 mmol, 0.1eq) in dry, degassed tetrahydrofuran (6 mL) was prepared. This solution was stirred for 5min to ensure the catalyst was fully dissolved during which time it turned deep red. Under inert conditions the solution of allyl boronic acid pinacol ester and *tert*-butyl cinnamyl carbonate was slowly added to the solution of Pd-catalyst. The reaction was heated under nitrogen at 60°C overnight. Upon completion, the reaction mixture was allowed to cool and diluted with diethyl ether. The mixture was filtered over a silica plug, washing with diethyl ether. The filtrate was evaporated under reduced pressure. The crude material was passed through a silica gel column (hexane) to yield the product as a colourless liquid (0.53g, 3.35mmol 60.4%).

^{1}H NMR (400 MHz, DMSO) δ 7.30 (t, J = 7.5 Hz, 2H, Ph-**H**), 7.23 – 7.15 (m, 3H, Ph-**H**), 6.03 – 5.89 (m, 1H, H_2C=**CH**-CHPh-CH_2-CH=CH_2), 5.75 – 5.60 (m, 1H, H_2C=CH-CHPh-CH_2-**CH**=CH_2), 5.05 – 4.89 (m, 4H **H_2C**=CH-CHPh-CH_2-CH=**CH_2**), 3.41 – 3.34 (m, 1H, H_2C=CH-**CH**Ph-CH_2-CH=CH_2), 2.48 – 2.39 (m, 2H, H_2C=CH-CHPh-**CH_2**-CH=CH_2).
^{13}C{^{1}H} NMR (101 MHz, DMSO) δ 143.53 (H_2C=CH-CH**Ph**-CH_2-CH=CH_2), 141.84 (H_2C=**C**H-CHPh-CH_2-CH=CH_2), 136.60 (H_2C=CH-CHPh-CH_2-**C**H=CH_2), 128.37 (H_2C=CH-CH**Ph**-CH_2-CH=CH_2), 127.53 (H_2C=CH-CH**Ph**-CH_2-CH=CH_2), 126.17 (H_2C=CH-CH**Ph**-CH_2-CH=CH_2), 116.34 (H_2**C**=CH-CHPh-CH_2-

CH=CH_2), 114.35 (H_2C=CH-CHPh-CH_2-CH=**C**H_2), 48.94 (H_2C=CH-**C**HPh-CH_2-CH=CH_2), 39.25 (H_2C=CH-CHPh-**CH_2**-CH=CH_2, overlapping with DMSO).

MS (es): +ve m/z calculated (158.24) found (158.1)

1-Phenyl-1,5-hexadiene

A solution of allyl boronic acid pinacol ester (1.40 g, 8.32 mmol, 1.3eq) and *tert*-butyl cinnamyl carbonate (1.50 g, 6.40 mmol, 1eq) in dry and degassed tetrahydrofuran (15 mL) was prepared. A separate solution of tris(dibenzylideneacteone)dipalladium(0) (0.293 g, 0.320mmol, 0.05eq) and 1,2-bis(diphenylphosphino)ethane (0.218 g, 0.832 mmol, 1.3eq) in dry, degassed tetrahydrofuran (7 mL) was prepared. Under inert conditions the solution of allyl boronic acid pinacol ester and *tert*-butyl cinnamyl carbonate was slowly added to solution of Pd-catalyst. The reaction was heated under nitrogen at 60^oC overnight. Upon completion the reaction was allowed to cool and diluted with diethyl ether. The mixture was filtered over a silica plug, washing with diethyl ether. The filtrate was evaporated under reduced pressure. The crude material was passed through a silica gel column (hexane) to yield the product as a colourless liquid (0.78g, 4.93mmol 77.0%).

^{1}H NMR (400 MHz, DMSO) δ 7.41 – 7.34 (m, 2H, **Ph**-CH=CH-CH_2-CH2-CH=CH_2), 7.30 (t, J = 7.6 Hz, 2H, **Ph**-CH=CH-CH_2-CH2-CH=CH_2), 7.23 – 7.16 (m, 1H, **Ph**-CH=CH-CH_2-CH2-CH=CH_2), 6.42 (d, J = 16.0 Hz, 1H, Ph-**CH**=CH-CH_2-CH2-CH=CH_2), 6.28 (dt, J = 15.9, 6.5 Hz, 1H, Ph-CH=**CH**-CH_2-CH2-CH=CH_2), 5.85 (ddt, J = 16.7, 10.2, 6.4 Hz, 1H, Ph-CH=CH-CH_2-CH_2-**CH**=CH_2), 5.12 – 4.95 (m, 2H, Ph-CH=CH-CH_2-CH2-CH=**CH_2**), 2.33 – 2.14 (m, 4H, Ph-CH=CH-**CH_2-CH_2**-CH=CH_2).
^{13}C{^{1}H} NMR (101 MHz, DMSO) δ 138.10 (Ph-CH=CH-CH_2-CH_2-**CH**=CH_2), 137.23 (**Ph**-CH=CH-CH_2-CH_2-CH=CH_2), 129.97 (Ph-**CH**=CH-CH_2-CH_2-CH=CH_2), 129.90 (**Ph**-CH=CH-CH_2-CH_2-CH=CH_2), 128.54 (2x **Ph**-CH=CH-CH_2-CH_2-CH=CH_2), 126.95, 125.82 (2x **Ph**-CH=CH-CH_2-CH_2-CH=CH_2), 115.20 (Ph-CH=CH-**CH_2-**CH_2-CH=**CH_2**), 32.99 (Ph-CH=CH-CH_2-**CH_2**-CH=CH_2), 31.78 (Ph-CH=CH-**CH_2-**CH_2-CH=CH_2).

MS (ES): +ve m/z calculated (158.24) found (158.1)

Section 2: Structure Generation, CREST Data and B3LYP Data Reactions A and B

Structures were built and optimised in the gas-phase at the B3LYP-D3BJ/6-311+G(d,p) level and subsequently optimised via GFN2-xTB using default parameters. Conformer searches were performed from the optimised-xTB structure using default parameters for the Conformer–Rotamer Ensemble Sampling Tool (CREST) within xTB version 6.4.1 at the GFN2-xTB level.[1,2] Subsequently the conformer/rotamer ensemble (CRE) sorting algorithm CREGEN was employed to isolate conformers from rotamers. Default thresholds were employed; energy 6 kcal/mol, RMSD 0.125 Å, conformer pairs 0.05 kcal/mol. If conformer sorting produced more than 50 conformers, the sort criteria for the RMSD value was altered in intervals of 0.5 (and smaller intervals in some cases) until ≈50 conformers were obtained.

The conformers obtained were subsequently optimized at the B3LYP-D3BJ/6-311-G+(d,p) level. Thus, not all conformers have been sampled at a higher level, but a proportion of the full range of accessible conformers has been examined. B3LYP conformers with identical or near identical energy were compared visually in Jmol[3] and the Jmol compare and rotate translate feature was used. This functionality compares two models and reorients the first model relative to the second based on a given atom-atom coordinate pairing or quaternion-based group-group orientation pairing.[4-6] Subsequently the lowest Gibbs Free energy conformer was used for the reaction energies, and where additional conformer analysis is undertaken conformers within 5 kJ/mol (at the B3LYP-D3BJ/6-311+G(d,p) level) of the lowest energy conformer were selected. In some cases the lowest G conformer differs from the lowest E conformer.

[1] CREST: Pracht, P.; Bohle, F.; Grimme, S.; *Phys. Chem. Chem. Phys.*, **2020**, 22, 7169-7192. DOI: 10.1039/C9CP06869D
[2] https://crest-lab.github.io/crest-docs/
[3] Jmol: an open-source Java viewer for chemical structures in 3D, http://www.jmol.org/
[4] Berthold K. P. Horn, *J. Opt. Soc. Amer. A*, **1987**, Vol. 4, pp. 629-64.
[5] G. R. Kneller, *Molecular Simulation*, **1991**, Vol. 7, pp. 113-119.
[6] https://chemapps.stolaf.edu/jmol/docs/#compare

Reaction A (Cope-Pr) Reactant

Rotamers & conformers: 434
default conformer search: 228
rthr=0.5 conformer search: 211
rthr=1.0 conformer search: 175
rthr=1.5 conformer search: 118
rthr=2.0 conformer search: 39 (selected)

No.	xTB Energy	Boltzmann	Probability		xTB No.	B3LYP ΔG	Boltzmann	Probability
	kJ/mol	exp(-ΔE/RT)	Q=4.73			kJ/mol	exp(-ΔG/RT)	Q=4.80
1	0.00	1.00	0.21		1	**0.00**	1.000	0.21
2	0.44	0.84	0.18		2	**0.44**	0.836	0.17
3	1.80	0.48	0.10		3	**1.88**	0.468	0.10
4	2.29	0.40	0.08		4	**2.34**	0.389	0.08
5	2.77	0.33	0.07		8	**2.58**	0.354	0.07
6	3.14	0.28	0.06		5	**2.88**	0.313	0.07
7	3.50	0.24	0.05		24	**3.26**	0.268	0.06
8	3.89	0.21	0.04		6	**3.27**	0.268	0.06
9	4.33	0.17	0.04		7	**3.38**	0.256	0.05
10	4.70	0.15	0.03		13	5.16	0.125	0.03
11	5.06	0.13	0.03		10	5.29	0.118	0.02
12	5.19	0.12	0.03		14	6.60	0.070	0.01
13	6.04	0.09	0.02		15	6.82	0.064	0.01
14	6.62	0.07	0.01		9	7.28	0.053	0.01
15	7.13	0.06	0.01		17	7.52	0.048	0.01
16	8.49	0.03	0.01		11	8.09	0.038	0.01
17	8.86	0.03	0.01		12	8.65	0.030	0.01
18	9.29	0.02	0.00		19	8.75	0.029	0.01
19	9.68	0.02	0.00		30	10.65	0.014	0.00
20	10.78	0.01	0.00		16	11.01	0.012	0.00
21	11.41	0.01	0.00		29	12.11	0.008	0.00
22	11.50	0.01	0.00		22	12.12	0.008	0.00
23	12.64	0.01	0.00		18	12.18	0.007	0.00
24	12.90	0.01	0.00		20	13.29	0.005	0.00
25	14.27	0.00	0.00		21	13.37	0.005	0.00
26	15.17	0.00	0.00		25	13.40	0.004	0.00
27	16.43	0.00	0.00		23	13.60	0.004	0.00
28	16.59	0.00	0.00		31	16.56	0.001	0.00
29	17.01	0.00	0.00		32	18.60	0.001	0.00
30	18.28	0.00	0.00		26	18.72	0.001	0.00
31	18.65	0.00	0.00		27	19.41	0.000	0.00
32	19.69	0.00	0.00		28	19.65	0.000	0.00
33	20.56	0.00	0.00		34	21.98	0.000	0.00
34	21.15	0.00	0.00		33	22.25	0.000	0.00
35	21.52	0.00	0.00		35	23.48	0.000	0.00
36	22.54	0.00	0.00		36	24.04	0.000	0.00
37	23.61	0.00	0.00		37	24.99	0.000	0.00
38	24.02	0.00	0.00		39	27.72	0.000	0.00
39	24.38	0.00	0.00		38	28.34	0.000	0.00

Table S2.1: Reaction A (Cope-Pr) reactant CREST data

Reaction A (Cope-Pr) Product

Rotamers & conformers: 580
default conformer search: 358
rthr=0.5 conformer search: 240
rthr=1.0 conformer search: 159
rthr=1.5 conformer search: 64
rthr=1.6 conformer search: 44 (selected)

No.	xTB Energy	Boltzmann	Probability		xTB No.	B3LYP ΔG	Boltzmann	Probability
	kJ/mol	exp(-ΔE/RT)	Q=7.89			kJ/mol	exp(-ΔG/RT)	Q=9.66
1	0.00	1.00	0.13		16	**0.00**	1.00	0.11
2	0.23	0.91	0.12		15	**0.42**	0.84	0.09
3	0.80	0.72	0.09		5	**0.82**	0.72	0.08
4	1.28	0.60	0.08		11	**1.03**	0.66	0.07
5	1.65	0.51	0.07		10	**1.69**	0.51	0.05
6	1.73	0.50	0.06		3	**1.69**	0.51	0.05
7	1.98	0.45	0.06		4	**1.70**	0.50	0.05
8	2.44	0.37	0.05		35	**1.97**	0.45	0.05
9	2.65	0.34	0.04		8	**2.52**	0.36	0.04
10	3.61	0.23	0.03		7	**2.70**	0.34	0.04
11	3.64	0.23	0.03		21	**2.92**	0.31	0.03
12	3.72	0.22	0.03		29	**3.21**	0.27	0.03
13	4.18	0.18	0.02		27	**3.38**	0.26	0.03
14	4.61	0.16	0.02		25	**3.53**	0.24	0.03
15	4.64	0.15	0.02		1	**3.70**	0.23	0.02
16	4.86	0.14	0.02		13	**3.70**	0.23	0.02
17	4.87	0.14	0.02		2	**3.70**	0.22	0.02
18	5.50	0.11	0.01		12	**3.84**	0.21	0.02
19	5.61	0.10	0.01		14	**4.03**	0.20	0.02
20	5.73	0.10	0.01		6	**4.36**	0.17	0.02
21	6.00	0.09	0.01		20	**4.52**	0.16	0.02
22	6.43	0.07	0.01		9	5.05	0.13	0.01
23	6.56	0.07	0.01		34	5.53	0.11	0.01
24	6.56	0.07	0.01		23	5.70	0.10	0.01
25	6.57	0.07	0.01		30	5.70	0.10	0.01
26	7.13	0.06	0.01		26	6.17	0.08	0.01
27	7.88	0.04	0.01		22	6.36	0.08	0.01
28	7.97	0.04	0.01		32	6.54	0.07	0.01
29	8.18	0.04	0.00		24	6.57	0.07	0.01
30	9.19	0.02	0.00		31	6.72	0.07	0.01
31	9.41	0.02	0.00		18	6.96	0.06	0.01
32	9.64	0.02	0.00		17	8.10	0.04	0.00
33	9.91	0.02	0.00		28	8.12	0.04	0.00
34	10.01	0.02	0.00		33	9.58	0.02	0.00
35	10.20	0.02	0.00		36	10.05	0.02	0.00
36	10.68	0.01	0.00		41	16.55	0.00	0.00
37	11.92	0.01	0.00		39	17.44	0.00	0.00
38	12.33	0.01	0.00		42	17.99	0.00	0.00
39	16.08	0.01	0.00		40	18.68	0.00	0.00
40	17.92	0.01	0.00		43	21.09	0.00	0.00
41	17.97	0.01	0.00		44	25.48	0.00	0.00
42	18.33	0.01	0.00					
43	20.47	0.01	0.00					
44	24.96	0.00	0.00					

Table S2.2: Reaction A (Cope-Pr) product CREST data

Reaction B (Cope-Ph) Reactant

Rotamers & conformers: 70
default conformer search: 41 (selected)
rthr=1.0 conformer search: 35

No.	xTB Energy	Boltzmann	Probability		xTB No.	B3LYP ΔG	Boltzmann	Probability
	kJ/mol	exp(-ΔE/RT)	Q=7.73			kJ/mol	exp(-ΔG/RT)	Q=8.36
1	0.00	1.00	0.13		2	**0.00**	1.00	0.12
2	0.26	0.90	0.12		25	**0.74**	0.74	0.09
3	1.11	0.64	0.08		1	**0.74**	0.74	0.09
4	1.31	0.59	0.08		7	**1.13**	0.63	0.08
5	1.35	0.58	0.07		3	**1.18**	0.62	0.07
6	1.54	0.54	0.07		8	**1.24**	0.61	0.07
7	1.95	0.45	0.06		11	**1.25**	0.60	0.07
8	2.13	0.42	0.05		5	**1.54**	0.54	0.06
9	2.56	0.36	0.05		6	**1.59**	0.53	0.06
10	2.71	0.34	0.04		4	**1.61**	0.52	0.06
11	3.58	0.24	0.03		9	**2.20**	0.41	0.05
12	3.64	0.23	0.03		10	**2.44**	0.37	0.04
13	4.37	0.17	0.02		18	**4.80**	0.14	0.02
14	4.46	0.17	0.02		22	**4.84**	0.14	0.02
15	4.49	0.16	0.02		15	5.08	0.13	0.02
16	5.21	0.12	0.02		16	5.35	0.12	0.01
17	5.48	0.11	0.01		14	5.83	0.10	0.01
18	5.49	0.11	0.01		24	6.08	0.09	0.01
19	5.77	0.10	0.01		12	6.61	0.07	0.01
20	5.88	0.09	0.01		17	7.08	0.06	0.01
21	6.20	0.08	0.01		23	7.56	0.05	0.01
22	6.43	0.07	0.01		19	7.68	0.05	0.01
23	7.41	0.05	0.01		20	7.86	0.04	0.01
24	7.50	0.05	0.01		34	8.40	0.03	0.00
25	8.32	0.03	0.00		27	9.36	0.02	0.00
26	9.12	0.03	0.00		30	14.29	0.00	0.00
27	9.50	0.02	0.00		33	14.73	0.00	0.00
28	10.18	0.02	0.00		40	19.55	0.00	0.00
29	10.21	0.02	0.00		38	20.04	0.00	0.00
30	12.42	0.01	0.00		41	21.91	0.00	0.00
31	12.62	0.01	0.00					
32	12.76	0.01	0.00					
33	12.79	0.01	0.00					
34	12.87	0.01	0.00					
35	13.82	0.00	0.00					
36	13.91	0.00	0.00					
37	15.23	0.00	0.00					
38	15.59	0.00	0.00					
39	16.82	0.00	0.00					
40	16.93	0.00	0.00					
41	17.78	0.00	0.00					

Table S2.3: Reaction B (Cope-Ph) reactant CREST data

Reaction B (Cope-Ph) Product

Rotamers & conformers: 132, rthr=0 conformer search: 69
rthr=0.5 conformer search: 58, rthr=1.0 conformer search: 49 *(selected)*

No.	xTB Energy	Boltzmann	Probability		xTB No.	B3LYP ΔG	Boltzmann	Probability
	kJ/mol	exp(-ΔE/RT)	Q=9.49			kJ/mol	exp(-ΔG/RT)	Q=12.29
1	0.00	1.00	0.11		2	**0.00**	1.00	0.08
2	0.88	0.70	0.07		12	**0.22**	0.92	0.07
3	0.89	0.70	0.07		24	**0.22**	0.91	0.07
4	1.41	0.57	0.06		8	**0.35**	0.87	0.07
5	1.79	0.49	0.05		14	**0.46**	0.83	0.07
6	1.79	0.49	0.05		19	**0.46**	0.83	0.07
7	1.89	0.47	0.05		31	**0.49**	0.82	0.07
8	2.02	0.44	0.05		29	**0.49**	0.82	0.07
9	2.08	0.43	0.05		4	**0.78**	0.73	0.06
10	2.09	0.43	0.05		1	**1.87**	0.47	0.04
11	2.12	0.42	0.04		11	**1.90**	0.46	0.04
12	2.37	0.38	0.04		15	**2.34**	0.39	0.03
13	2.43	0.38	0.04		18	**2.57**	0.35	0.03
14	2.57	0.35	0.04		28	**2.90**	0.31	0.03
15	3.27	0.27	0.03		21	**2.90**	0.31	0.03
16	3.28	0.27	0.03		42	**2.96**	0.30	0.02
17	4.39	0.17	0.02		17	**2.96**	0.30	0.02
18	5.07	0.13	0.01		9	**3.27**	0.27	0.02
19	5.13	0.13	0.01		10	**3.28**	0.27	0.02
20	5.32	0.12	0.01		40	**3.84**	0.21	0.02
21	5.41	0.11	0.01		35	**3.84**	0.21	0.02
22	5.58	0.11	0.01		22	**4.16**	0.19	0.02
23	5.99	0.09	0.01		23	**4.16**	0.19	0.02
24	6.02	0.09	0.01		39	5.50	0.11	0.01
25	6.54	0.07	0.01		26	5.50	0.11	0.01
26	6.82	0.06	0.01		48	8.14	0.04	0.00
27	6.90	0.06	0.01		46	8.14	0.04	0.00
28	7.15	0.06	0.01		38	10.37	0.02	0.00
29	7.16	0.06	0.01		37	10.37	0.02	0.00
30	7.18	0.06	0.01					
31	7.26	0.05	0.01					
32	7.28	0.05	0.01					
33	7.45	0.05	0.01					
34	7.65	0.05	0.00					
35	8.63	0.03	0.00					
36	8.87	0.03	0.00					
37	9.49	0.02	0.00					
38	9.97	0.02	0.00					
39	10.36	0.02	0.00					
40	10.72	0.01	0.00					
41	10.83	0.01	0.00					
42	11.16	0.01	0.00					
43	11.24	0.01	0.00					
44	11.39	0.01	0.00					
45	11.75	0.01	0.00					
46	11.92	0.01	0.00					
47	12.15	0.01	0.00					
48	12.51	0.01	0.00					
49	13.41	0.00	0.00					

Table S2.4: Reaction B (Cope-Ph) product CREST data

Section 3. TS Conformers

A starting TS structure was obtained by forming a chair-equatorial conformer and positioning the reactive atoms in a TS like geometry. The structures was then optimised to a transition state using the Berny algorithm. The TS was confirmed by a frequency analysis and visual inspection of the negative (imaginary) mode to confirm the correct TS had been located. IRC scans were performed to confirm the formation of the desired product from the TS.

The TS can take on a boat or chair arrangement of the interacting atoms, in addition the Pr or Ph substituent can take on an equatorial or axial configuration, leading to 4 potential isomers for each Cope reaction, **Figure 4** in the paper. The optimised chair-equatorial TS conformer was altered to a boat form and a fully relaxed TS search performed. Both conformers were then altered to the axial conformer and a fully relaxed TS search was performed.

There is also potential for rotation of the substituents. Rotation of the phenyl substituent was evaluated for the GP equatorial chair TS conformer, the reacting atoms where fixed in place and the dihedral for the phenyl ring rotated. The rotation started from the optimised conformer which has a C-C-C-C_{Ph} dihedral of 31º, the energy was evaluated at steps of 20º, and a maximum energy barrier of 25 kJ/mol was determined, **Figure S3.1**. Thus the initially obtained optimised conformers are confirmed as the local minima structures.

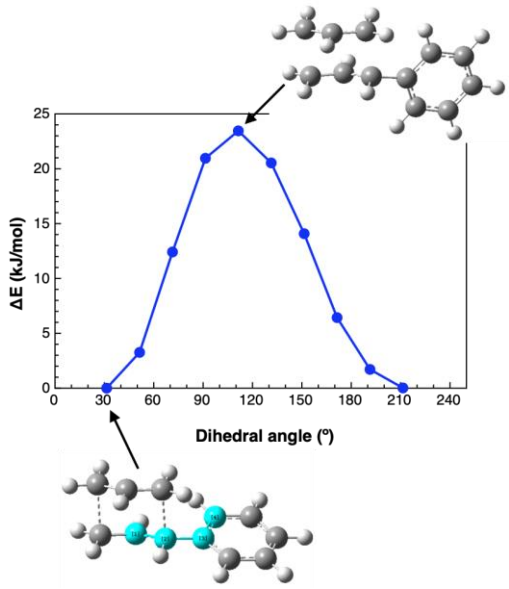

Figure S3.1: Rotational potential energy surface of the Ph substituent for the gas phase Cope-Ph transition state at the B3LYP-D3BJ/6-311+G(d,p) level.

Cope-Pr	B3LYP				M06-2X			
ΔE_{TS}	chair equatorial	chair axial	boat equatorial	boat axial	chair equatorial	chair axial	boat equatorial	boat axial
Gas Phase	0	6	32	32	0	11	47	43
MeCN	0	6	31	31	0	6	43	43
Benzene	0	6	32	32	0	7	44	44
Ethanol	0	6	32	31	0	6	44	44
$[C_4C_1im][NTf_2]$	0	6	32	31	0	6	44	44

Table S3.1: Reaction A (Cope-Pr) energy difference (kJ/mol) between the TS conformers, $\Delta E_{TS}=E_x-E_{chair\text{-}Req}$.

Cope-Pr	B3LYP				M06-2X			
ΔG_{TS}	chair equatorial	chair axial	boat equatorial	boat axial	chair equatorial	chair axial	boat equatorial	boat axial
Gas Phase	0	6	27	29	0	9	40	40
MeCN	0	6	26	29	0	7	38	40
Benzene	0	6	27	30	0	8	39	41
Ethanol	0	6	27	29	0	8	39	41
$[C_4C_1im][NTf_2]$	0	6	27	29	0	7	39	41

Table S3.2: Reaction A (Cope-Pr) energy difference (kJ/mol) between the TS conformers, $\Delta G_{TS}=G_x-G_{chair\text{-}Req}$.

Cope-Pr	B3LYP		M06-2X
$\Delta G_{TS}=G_{boat\text{-}Req}-G_{chair\text{-}Req}$	$\Delta G_{TS,298}$	$\Delta G_{TS,423}$	$\Delta G_{TS,298}$
Gas Phase	6	6	9
MeCN	6	5	7
Benzene	6	6	8
Ethanol	6	6	8
$[C_4C_1im][NTf_2]$	6	6	7

Table S3.3: Reaction A (Cope-Pr) Gibbs Free Energy difference (kJ/mol) between the TS *chair* equatorial and axial conformers, $\Delta G_{TS}= G_{Rax}-G_{Req}$ at 298.15K and 423.15K.

Cope-Pr	B3LYP		M06-2X
$\Delta G_{TS}=G_{boat\text{-}Req}-G_{chair\text{-}Req}$	$\Delta G_{TS,298}$	$\Delta G_{TS,423}$	$\Delta G_{TS,298}$
Gas Phase	27	26	40
MeCN	29	25	40
Benzene	30	26	41
Ethanol	29	26	41
$[C_4C_1im][NTf_2]$	29	26	41

Table S3.4: Reaction A (Cope-Pr) Gibbs Free Energy difference (kJ/mol) between the TS *equatorial* boat and chair conformers, $\Delta G_{TS}= G_{boat}-G_{chair}$ at 298.15K and 423.15K.

Cope-Ph	B3LYP				M06-2X			
ΔE_{TS}	chair equatorial	chair axial	boat equatorial	boat axial	chair equatorial	chair axial	boat equatorial	boat axial
Gas Phase	0	16	25	40	0	21	37	53
MeCN	0	17	25	41	0	17	42	54
Benzene	0	17	25	41	0	16	38	55
Ethanol	0	17	25	41	0	17	38	54
$[C_4C_1im][NTf_2]$	0	17	25	41	0	16	38	54

Table S3.5: Reaction B (Cope-Ph) energy difference (kJ/mol) between the TS conformers, $\Delta E_{TS}=E_x-E_{chair\text{-}Req}$.

Cope-Ph	B3LYP				M06-2X			
ΔG_{TS}	chair equatorial	chair axial	boat equatorial	boat axial	chair equatorial	chair axial	boat equatorial	boat axial
Gas Phase	0	17	21	37	0	20	32	52
MeCN	0	17	21	37	0	19	34	52
Benzene	0	17	20	39	0	18	33	55
Ethanol	0	16	21	37	0	19	33	51
$[C_4C_1im][NTf_2]$	0	16	21	37	0	19	33	51

Table S3.6: Reaction B (Cope-Ph) energy difference (kJ/mol) between the TS conformers, $\Delta G_{TS}=G_x-G_{chair\text{-}Req}$.

Cope-Ph	B3LYP		M06-2X
$\Delta G_{TS}=G_{boat\text{-}Req}-G_{chair\text{-}Req}$	$\Delta G_{TS,298}$	$\Delta G_{TS,423}$	$\Delta G_{TS,298}$
Gas Phase	17	17	20
MeCN	17	16	19
Benzene	17	18	18
Ethanol	16	16	19
$[C_4C_1im][NTf_2]$	16	16	19

Table S3.7: Reaction B (Cope-Ph) Gibbs Free Energy difference (kJ/mol) between the TS *chair* equatorial and axial conformers, $\Delta G_{TS}= G_{Rax}-G_{Req}$ at 298.15K and 423.15K. B3LYP=B3LYP-D3BJ/6-311-G+(d,p), M06-2X= M06-2X-D3/6-311-G+(d,p)

Cope-Ph	B3LYP		M06-2X
$\Delta G_{TS}=G_{boat(equatorial)}-G_{chair(equatorial)}$	$\Delta G_{TS,298}$	$\Delta G_{TS,423}$	$\Delta G_{TS,298}$
Gas Phase	21	20	32
MeCN	21	20	34
Benzene	20	18	33
Ethanol	21	20	33
$[C_4C_1im][NTf_2]$	21	20	33

Table S3.8: Reaction B (Cope-Ph) Gibbs Free Energy difference (kJ/mol) between the TS *equatorial* boat and chair conformers, $\Delta G_{TS}= G_{boat}-G_{chair}$ at 298.15K and 423.15K. B3LYP=B3LYP-D3BJ/6-311-G+(d,p), M06-2X= M06-2X-D3/6-311-G+(d,p)

Section 4. Reaction Energies

$\Delta E(TS)=E_{TS}-E_{reactants}$ and $\Delta E(Reaction)=E_{products}-E_{reactants}$

Reaction A (Cope-Pr)

B3LYP		TS				Reaction		
	ΔE	ΔG	ΔH	TΔS	ΔE	ΔG	ΔH	TΔS
Gas Phase	132	135	126	-10	-3	-4	-1	4
MeCN	130	134	124	-10	-7	-8	-4	4
Benzene	131	135	125	-10	-7	-8	-4	4
Ethanol	129	134	123	-10	-7	-7	-4	4
$[C_4C_1im][NTf_2]$	130	134	124	-10	-7	-7	-4	3

Table S4.1: Reaction A (Cope-Pr) **B3LYP**-D3BJ/6-311-G+(d,p) thermochemical data (kJ/mol) at 298.15K.

M06-2X		TS				Reaction		
	ΔE	ΔG	ΔH	TΔS	ΔE	ΔG	ΔH	TΔS
Gas Phase	144	150	139	-11	2	0	4	3
MeCN	141	147	136	-11	-3	-4	-1	3
Benzene	141	148	137	-12	-3	-4	-1	3
Ethanol	140	146	135	-11	-3	-4	-1	3
$[C_4C_1im][NTf_2]$	140	147	136	-12	-3	-4	-1	3

Table S4.2: Reaction A (Cope-Pr) **M06-2X**-D3/6-311+G(d,p) thermochemical data (kJ/mol) at 298.15K.

Reaction B (Cope-Ph)

B3LYP		TS				Reaction		
	ΔE	ΔG	ΔH	TΔS	ΔE	ΔG	ΔH	TΔS
Gas Phase	118	120	111	-9	-11	-11	-10	1
MeCN	116	120	110	-10	-14	-13	-13	0
Benzene	116	120	110	-10	-15	-14	-12	0
Ethanol	115	119	109	-10	-14	-13	-13	0
$[C_4C_1im][NTf_2]$	115	119	109	-10	-15	-13	-14	-1

Table S4.3: Reaction B (Cope-Ph) **B3LYP**-D3BJ/6-311-G+(d,p) thermochemical data (kJ/mol) at 298.15K.

M06-2X		TS				Reaction		
	ΔE	ΔG	ΔH	TΔS	ΔE	ΔG	ΔH	TΔS
Gas Phase	134	138	128	-10	-9	-8	-8	0
MeCN	130	136	125	-11	-12	-10	-11	-1
Benzene	131	136	125	-10	-13	-12	-12	0
Ethanol	129	135	124	-11	-13	-11	-12	-1
$[C_4C_1im][NTf_2]$	129	135	124	-11	-13	-11	-12	0

Table S4.4: Reaction B (Cope-Ph) **M06-2X**-D3/6-311+G(d,p) l thermochemical data (kJ/mol) at 298.15K

High Temperature

Reaction A (Cope-Pr)	TS ΔE	TS ΔG	TS ΔH	TS TΔS	Reaction ΔE	Reaction ΔG	Reaction ΔH	Reaction TΔS
Gas Phase	132	140	126	-15	-3	-8	-1	6
MeCN	130	139	124	-15	-7	-9	-6	4
Benzene	131	140	125	-15	-7	-10	-6	4
Ethanol	129	139	123	-15	-7	-9	-5	4
$[C_4C_1im][NTf_2]$	130	139	124	-15	-7	-10	-6	4

Table S4.5: Reaction A (Cope-Pr) **B3LYP**-D3BJ/6-311-G+(d,p) thermochemical data (kJ/mol) at **423.15K**.

Reaction B (Cope-Ph)	TS ΔE	TS ΔG	TS ΔH	TS TΔS	Reaction ΔE	Reaction ΔG	Reaction ΔH	Reaction TΔS
Gas Phase	118	126	114	-11	-11	-10	-7	3
MeCN	116	125	110	-15	-14	-13	-14	-1
Benzene	116	125	110	-15	-15	-14	-15	-1
Ethanol	115	124	109	-14	-14	-13	-14	-1
$[C_4C_1im][NTf_2]$	115	125	109	-16	-15	-12	-14	-2

Table S4.6: Reaction B (Cope-Ph) **B3LYP**-D3BJ/6-311-G+(d,p) thermochemical data (kJ/mol) at **423.15K**.

DFT check

Functional	TS ΔE	TS ΔG	Benchmark RMSD (ref 42)
B3LYP-D3BJ	118	120	6.3
M06-2X-D3	134	138	7.5
M06-L	125	123	8.8
PBE0	153	139	14.6*

Table S4.7: Reaction B (Cope-Ph) in the gas-phase **DFT functionals** (6-311+G(d,p) basis) barrier energy and Gibbs Free Energy (kJ/mol) at 298.15K. Benchmark root mean square deviations (RMSD) in kJ/mol from ref 42 (of the paper) ESI Table S6, *the benchmark study included a D3BJ dispersion correction

Section 5. Solvation Energies

Reaction A (Cope-Pr)

B3LYP	Reactant	TS Chair eq	Product	E_a
Gas Phase	0	0	0	0
MeCN	-21	-22	-25	-2
Benzene	-22	-23	-26	-2
Ethanol	-18	-21	-23	-3
$[C_4C_1im][NTf_2]$	-14	-17	-19	-2

Table S5.1: Solvation Energies ΔE (kJ/mol) for reaction A at 298.15K, **B3LYP**-D3BJ/6-311-G+(d,p).

M06-2X	Reactant	TS Chair eq	Product	E_a
Gas Phase	0	0	0	0
MeCN	-22	-26	-26	-3
Benzene	-22	-25	-26	-3
Ethanol	-20	-25	-24	-4
$[C_4C_1im][NTf_2]$	-16	-20	-20	-4

Table S5.2: Solvation Energies ΔE (kJ/mol) for reaction A at 298.15K, **M06-2X**-D3/6-311+G(d,p).

Reaction B (Cope-Ph)

B3LYP	Reactant	TS	Product	E_a
Gas Phase	0	0	0	0
MeCN	-35	-37	-39	-2
Benzene	-31	-33	-36	-2
Ethanol	-29	-32	-33	-3
$[C_4C_1im][NTf_2]$	-26	-29	-30	-2

Table S5.3: Solvation Gibbs Free Energies ΔG (kJ/mol) for reaction A at 298.15K, **B3LYP**-D3BJ/6-311+G(d,p).

M06-2X	Reactant	TS	Product	E_a
Gas Phase	0	0	0	0
MeCN	-39	-42	-42	-3
Benzene	-33	-36	-37	-3
Ethanol	-33	-37	-37	-4
$[C_4C_1im][NTf_2]$	-30	-34	-34	-4

Table S5.4 Solvation Gibbs Free Energies ΔG (kJ/mol) for reaction A at 298.15K, **M06-2X**-D3/6-311+G(d,p).

Section 6: Structure Generation, CREST Data and B3LYP Data Reaction C

Reaction C (Cope-diPh) reactant

Rotamers & conformers: 164
rthr=0 conformer search: 69
rthr=0.5 conformer search: 55
rthr=1.0 conformer search: 51
rthr=2.0 conformer search: 40 (selected)

No.	xTB Energy	Boltzmann	Probability		xTB No.	B3LYP Gibbs Free Energy	Boltzmann	Probability
	kJ/mol	exp(-ΔE/RT)	Q=3.89			kJ/mol	exp(-ΔG/RT)	Q=2.10
1	0.00	1.00	0.26		1	**0.00**	1.000	0.48
2	1.11	0.64	0.16		2	**1.62**	0.521	0.25
3	1.49	0.55	0.14		5	**3.55**	0.239	0.11
4	2.35	0.39	0.10		4	5.91	0.092	0.04
5	3.39	0.25	0.07		9	7.24	0.054	0.03
6	3.61	0.23	0.06		11	7.31	0.052	0.02
7	3.87	0.21	0.05		7	7.60	0.047	0.02
8	4.46	0.17	0.04		10	8.22	0.036	0.02
9	6.05	0.09	0.02		14	9.86	0.019	0.01
10	6.78	0.06	0.02		25	9.86	0.019	0.01
11	7.17	0.06	0.01		29	12.52	0.006	0.00
12	7.45	0.05	0.01		16	14.01	0.004	0.00
13	7.88	0.04	0.01		31	14.71	0.003	0.00
14	8.96	0.03	0.01		37	15.47	0.002	0.00
15	9.51	0.02	0.01		27	15.47	0.002	0.00
16	10.39	0.02	0.00		30	15.83	0.002	0.00
17	10.71	0.01	0.00		24	15.83	0.002	0.00
18	10.95	0.01	0.00		26	16.27	0.001	0.00
19	11.44	0.01	0.00		35	19.84	0.000	0.00
20	11.44	0.01	0.00		32	20.35	0.000	0.00
21	12.06	0.01	0.00		33	21.11	0.000	0.00
22	12.29	0.01	0.00		38	27.68	0.000	0.00
23	12.92	0.01	0.00					
24	13.38	0.00	0.00					
25	13.95	0.00	0.00					
26	14.75	0.00	0.00					
27	15.07	0.00	0.00					
28	15.24	0.00	0.00					
29	17.30	0.00	0.00					
30	17.51	0.00	0.00					
31	18.07	0.00	0.00					
32	18.21	0.00	0.00					
33	18.62	0.00	0.00					
34	19.26	0.00	0.00					
35	19.65	0.00	0.00					
36	19.81	0.00	0.00					
37	20.15	0.00	0.00					
38	23.04	0.00	0.00					
39	24.15	0.00	0.00					
40	24.56	0.00	0.00					

Table S6.1: Reaction C (Cope-diPh) reactant CREST data

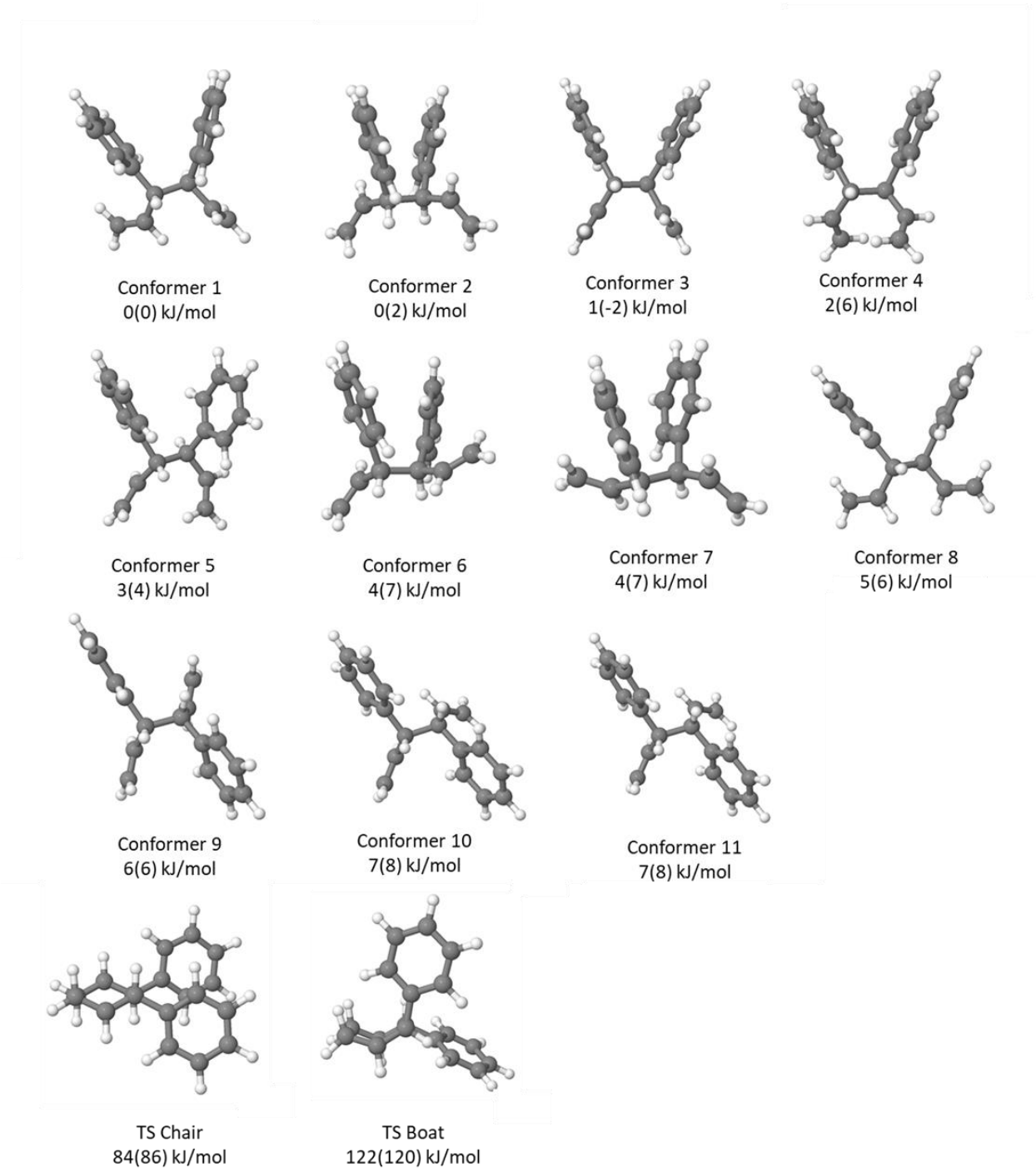

Figure S6.1 Reaction C reactant and TS conformers B3LYP-D3BJ/6-311+G(d,p) with relative energies ΔE(ΔG).

Section 7: AIMALL and Jmol Volume Data

CREST derived conformers, re-optimised at the B3LYP-D3BJ/6-311+G(d,p) level, those under 5 and 10 kJ/mol kJ/mol were analysed. AIMALL: Wfn files were generated and QTAIM analysis carried out. The volume from the 0.001 isodensity surfaces was extracted. JMol: The optimised log files were imported into JMol. The 0 radius of the solvent excluded surface was evaluated (this is essentially the smoothed VdW surface) using the command "isosurface resolution 20 volume solvent 0".

AIMALL and JMol Volumes

Conformer	Energy (kJ/mol)	AIMALL Vol cm^3/mol	JMol Vol cm^3/mol
1	**0.00**	**205.01**	**231.42**
2	0.13	204.33	231.6
3	0.51	205.95	231.48
4	2.20	203.83	231.31
5	3.35	204.75	231.4
6	3.64	203.69	231.41
7	3.64	203.70	231.41
8	4.70	204.26	231.35
9	6.09	205.14	231.79
10	7.20	204.47	231.56
11	7.20	204.47	231.56
AVG	< 5 kJ/mol	**204.4 ± 0.7**	231.42 ± 0.08
AVG	< 10 kJ/mol	204.5 ± 0.7	231.48 ± 0.1
TS Chair-$R_{eq,eq}$	84.39	**203.28**	231.17
TS Boat-$R_{eq,ax}$	122.04	204.62	231.65
ΔV(conf 1)	0.00	**-1.73**	-0.26
ΔV(AVG)	< 5 kJ/mol	**-1.2 ± 0.7**	-0.25

Table S7.1 Reaction C, relative energy ΔE(kJ/mol) to the lowest energy structure, and determined volume (cm^3/mol) for each conformer using AIMALL and JMol.

Conformer	Energy (kJ/mol)	AIMALL Vol cm^3/mol	JMol Vol cm^3/mol	r(C^1-C^6) Å
1	0.00	**146.8**	162.71	5.33
2	0.49	146.8	162.76	6.04
3	0.49	146.8	162.76	6.03
4	0.91	147.5	162.83	5.60
5	1.64	147.0	162.69	5.40
6	1.70	146.9	162.74	5.87
7	2.19	146.8	162.79	5.87
8	2.40	147.6	162.86	4.77
9	2.68	147.7	162.81	5.96
10	2.68	147.7	162.81	5.96
11	3.96	146.9	162.83	4.68
12	4.11	146.9	162.82	4.82
13	4.36	146.0	162.62	5.55
14	4.41	147.7	162.84	4.30
15	4.92	146.2	162.8	5.11
16	4.95	146.8	162.81	5.56
17	4.99	146.8	162.79	3.73
18	5.20	146.1	162.8	3.72
19	5.31	146.7	162.7	5.37
20	5.88	146.2	162.76	3.48
21	5.92	146.3	162.77	4.68
22	6.14	146.9	162.92	5.45
23	6.14	146.9	162.92	5.45
24	6.68	146.3	162.85	4.58
25	7.69	146.1	162.69	5.33
26	8.53	146.8	162.84	3.71
AVG	< 5 kJ/mol	**147.0 ± 0.5**	162.78 ± 0.06	
AVG	< 10 kJ/mol	146.8 ± 0.5	162.79 ± 0.07	
TS Chair-R_{eq}	118.21	**145.1**	162.2	2.20
TS Chair-R_{ax}	134.48	144.1	162.2	2.22
TS Boat-R_{eq}	144.07	146.3	163.5	2.36
TS Boat-R_{ax}	158.39	145.3	163.5	2.39
ΔV(conf 1)	0.00	**-1.75**	**-0.50**	
ΔV(AVG)	< 5 kJ/mol	**-1.9 ± 0.5**	**-0.60 ± 0.06**	

Table S7.2 Reaction B, relative energy ΔE(kJ/mol) to the lowest energy structure, and determined volume (cm^3/mol) for each conformer using AIMALL and JMol.

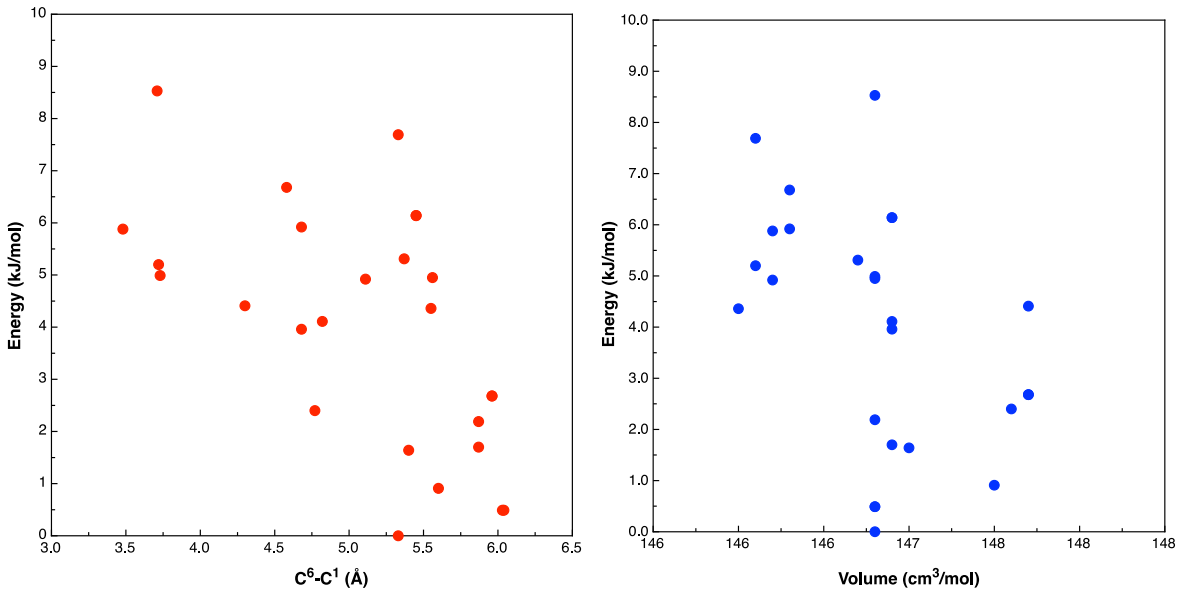

(a) (b)

Figure S7.2 (a) r(C^1-C^6) vs energy and (b) AIMALL volume vs energy for reaction B conformers.

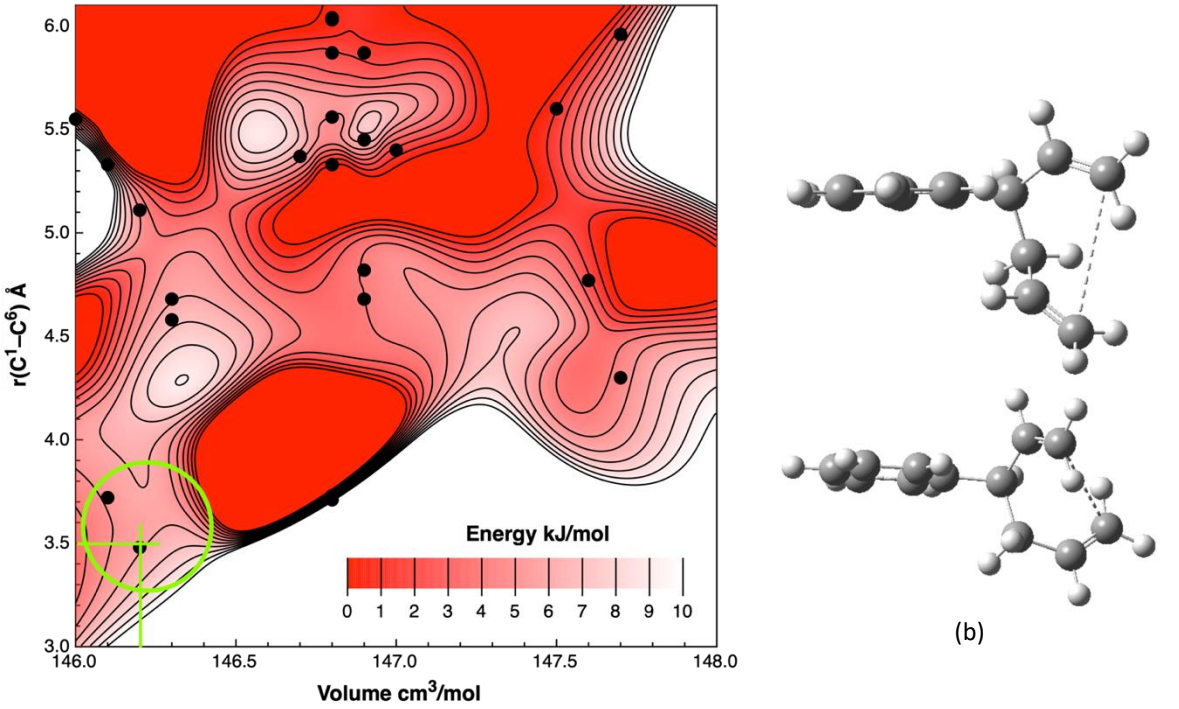

(a) (b)

Figure S7.3 (a) r(C^1-C^6) vs volume, with z-axis as energy, data used to interpolate a contour map for reaction B conformers, shortest r(C^1-C^6) and smallest volume conformers emphasises in green, (b) the two structures with the "optimal" volume/r(C-C) ratio.

Section 8: Structures for TS-solvent cluster analysis

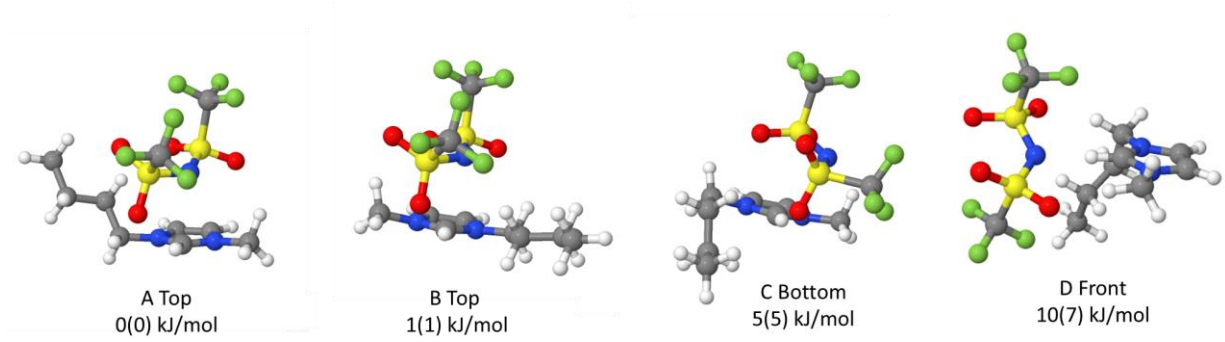

Figure S8.1: Low energy structures of B3LYP-D3BJ/6-311+G(d,p) [C_4C_1im][NTf_2] with relative energies ΔE(ΔG) in kJ/mol.

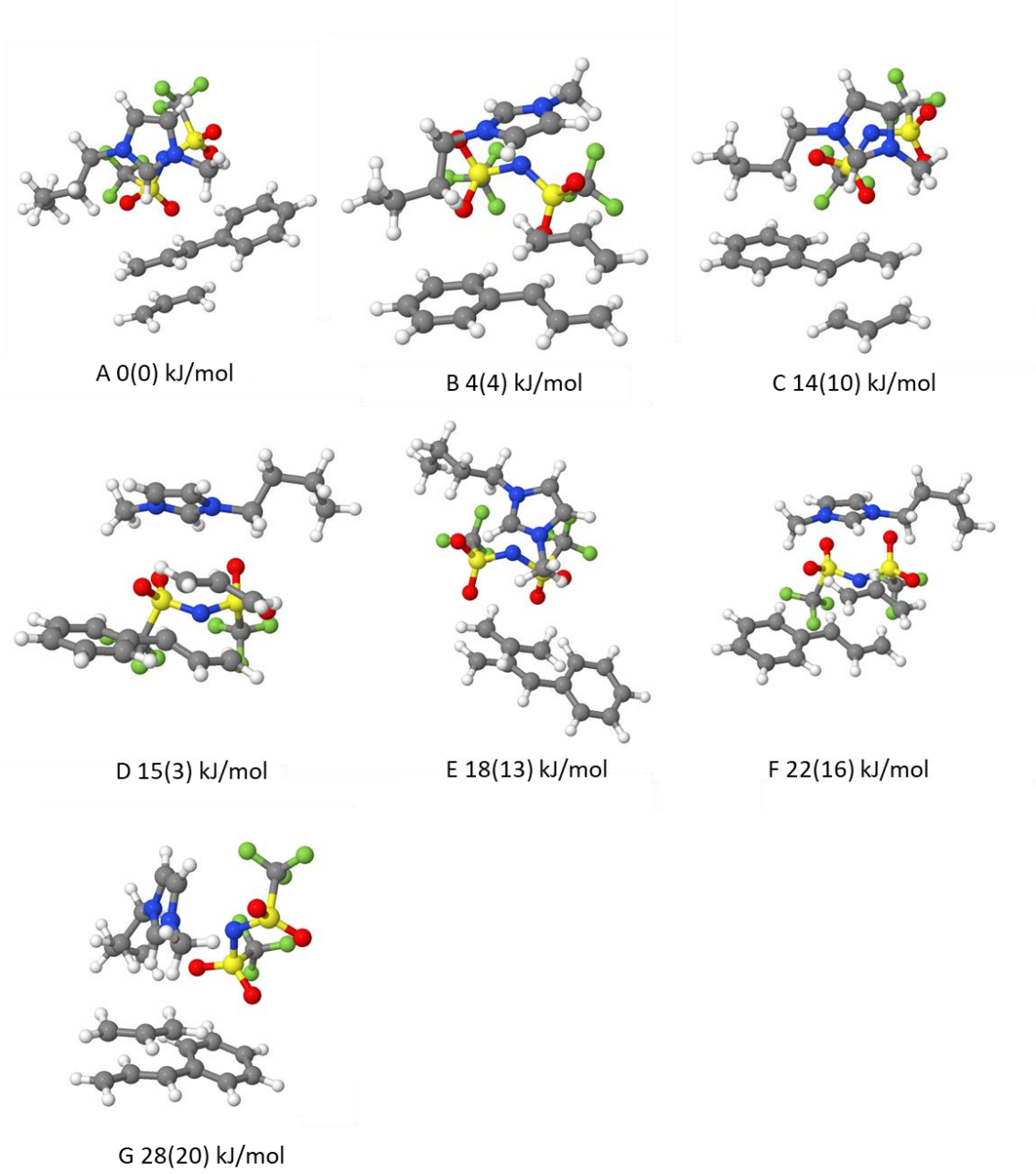

Figure S8.2: Low energy structures of [C_4C_1im][NTf_2] interacting with TS Chair (equatorial) B3LYP-D3BJ/6-311+G(d,p), ΔE(ΔG) in kJ/mol.

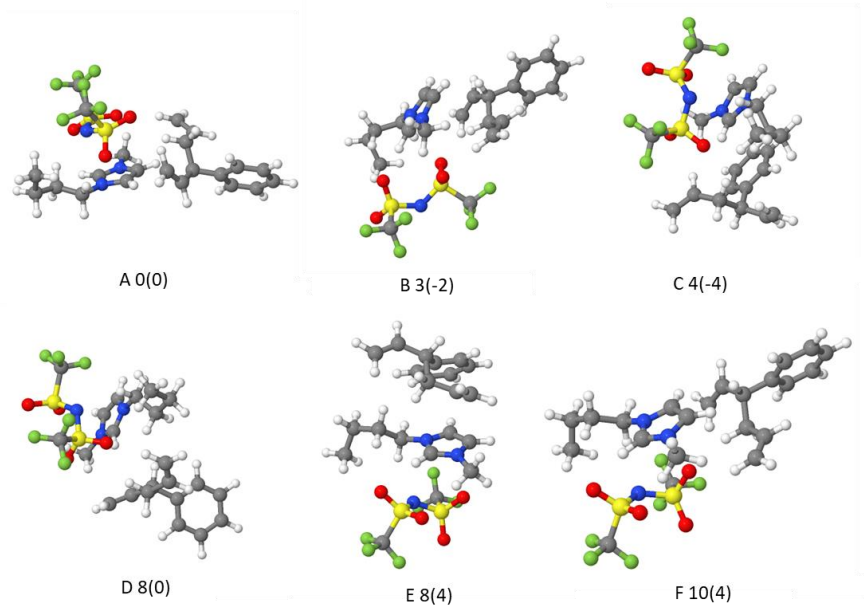

Figure 8.*3*: Low energy structures of $[C_4C_1im][NTf_2]$ interacting with the reactant B3LYP-D3BJ/6-311+G(d,p), ΔE(ΔG) in kJ/mol.

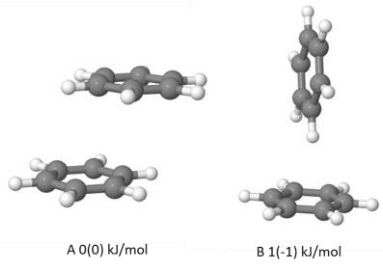

Figure S8.*4*: Low energy structures of two benzene molecules B3LYP-D3BJ/6-311+G(d,p), ΔE(ΔG) in kJ/mol.

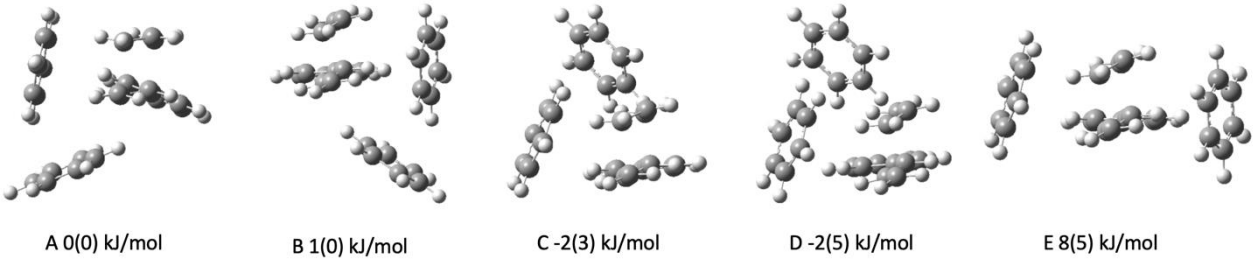

Figure S8.5: Low energy structures of two benzene molecules interacting with TS Chair (eq) B3LYP-D3BJ/6-311+G(d,p), ΔE(ΔG) in kJ/mol.

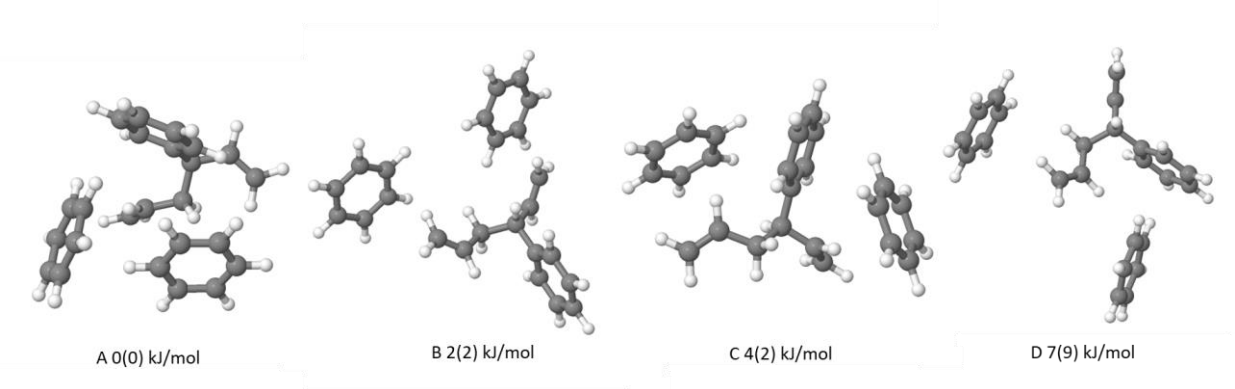

Figure 8.6: Low energy structures of two benzene molecules interacting with the reactant B3LYP-D3BJ/6-311+G(d,p) , ΔE(ΔG) in kJ/mol.

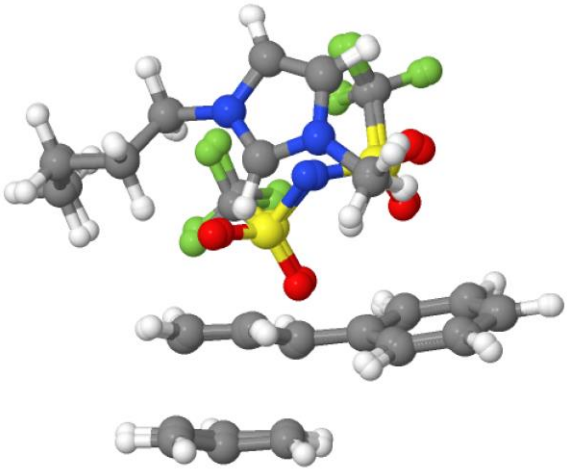

Figure 8.6: Low energy structures of two benzene molecules interacting with the reactant B3LYP-D3BJ/6-311+G(d,p) , ΔE(ΔG) in kJ/mol.

Section 9: Association Energy of TS-solvent clusters

method	React-B ΔE	React-B ΔH	React-B ΔG	TS-B ΔE	TS-B ΔH	TS-B ΔG
IP E_{ass} (kJ/mol)						
B3LYP	-37	-30	+14	-59	-52	0
B3LYP-ILSMD	-27	-22	+30	-40	-33	+21
M06-2X	-47	-41	+11	-67	-61	-8
2Bz E_{ass} (kJ/mol)						
B3LYP	-39	-32	+26	-45	-38	+17
B3LYP -BzSMD	-30	-24	+26	-30	-25	+21
M06-2X	-48	-42	+16	-49	-43	+16

Table S9.1 Solvent association energy $E_{ass}=E_{cluster}-(E_{TS}+E_{solvent})$ in the gas-phase, at the B3LYP, M06-2X level for reaction B.

(a) (b)

Figure S9.1 Overlay of the cluster structures in the gas-phase and respective SMD environments (a) TS-IL in ILSMD and (b)TS-2Bz in BzSMD.

Section 10: AIM Analysis of TS-solvent clusters

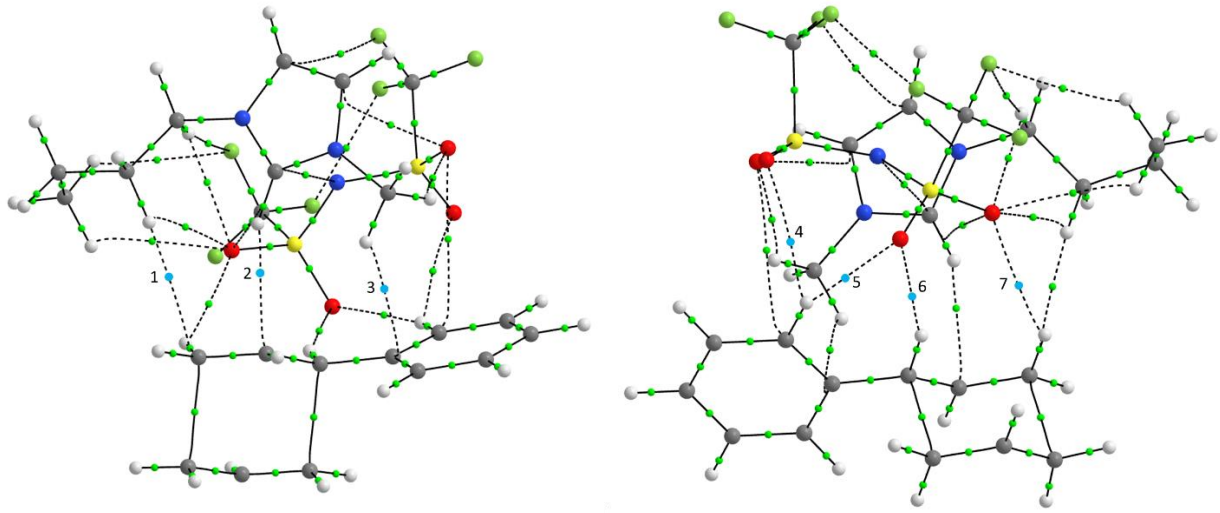

Figure S10.1 AIM analysis of B3LYP-D3BJ/6-311+G(d,p) TS-IL showing BCPs between the cation (left) and the anion (right) and the TS Chair (eq). Relevant BCPs highlighted in blue.

Number	Connecting atoms	ρ(r)-GP	$\nabla^2\rho(r)$	ρ(r)-IL
1	H-H	0.005	0.015	0.005
2	H-C	0.009	0.023	0.008
3	H-C	0.008	0.027	0.007
4	O-H	0.005	0.016	-
5	O-H	0.011	0.035	0.010
6	O-H	0.011	0.035	0.007
7	O-H	0.007	0.025	0.005

Table S10.1 Electron density and the Laplacian for selected bond critical points of the gas-phase B3LYP-D3BJ/6-311+G(d,p) TS-IL structure and the TS-IL structure within the IL-SMD.

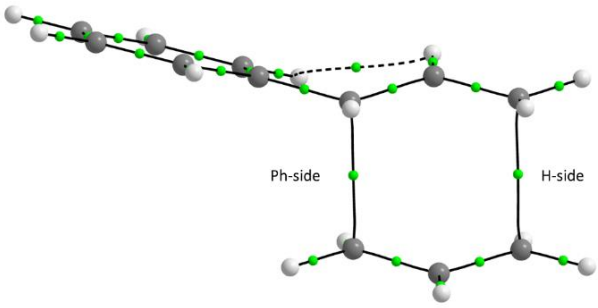

Figure S9.2 Selected bond critical points for the B3LYP-D3BJ/6-311+G(d,p) TS Chair (eq).

Both BCPs involved in bond breaking/forming shower higher electron density when bound to the IL

Number	Connecting atoms	ρ(r)	$\nabla^2\rho(r)$
		Just TS Chair	
1 (H-Side)	C-C	0.055	0.043
2 (Ph-Side)	C-C	0.063	0.033
		TS Chair + IL	
1 + IL (H-Side)	C-C	0.057	0.042
2 + IL (Ph-Side)	C-C	0.065	0.033

Table S10.2 Electron density and the Laplacian for selected bond critical points of the isolated gas-phase B3LYP-D3BJ/6-311+G(d,p) TS.

Section 11: NCI plots of TS-solvent clusters

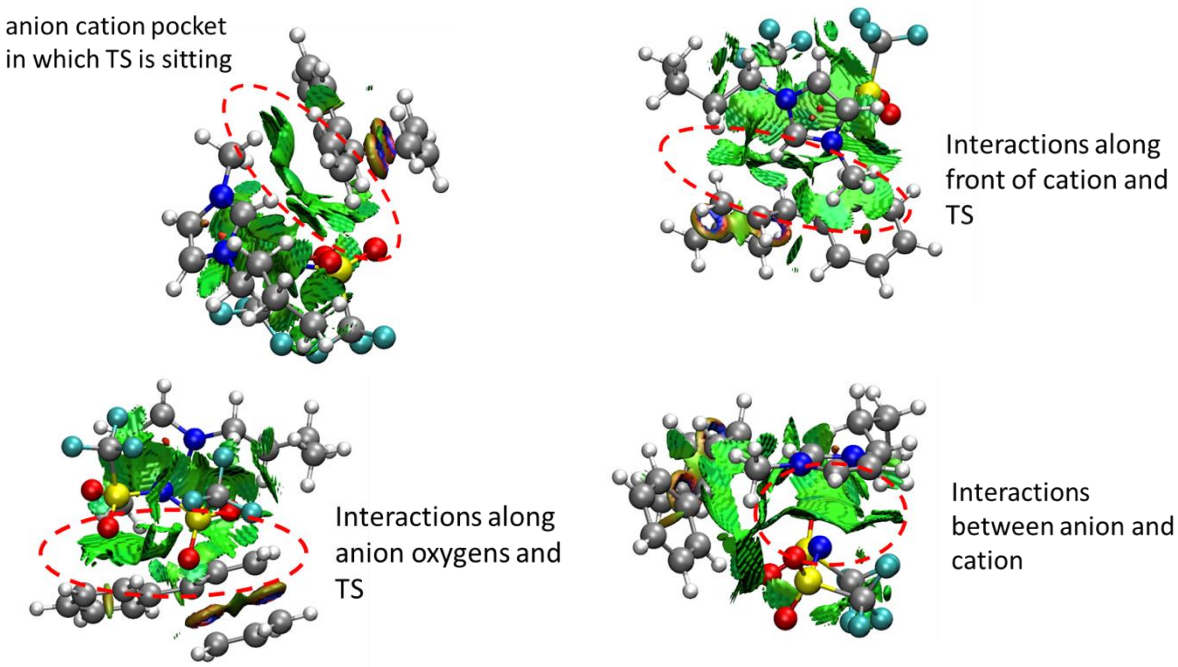

Figure S11.1 NCI plot of $[C_4C_1im][NTf_2]$ interacting with the TSChair equatorial*, B3LYP-D3BJ/6-311+G(d,p)*

Section 12: NBO and CHelpG Charge Analysis

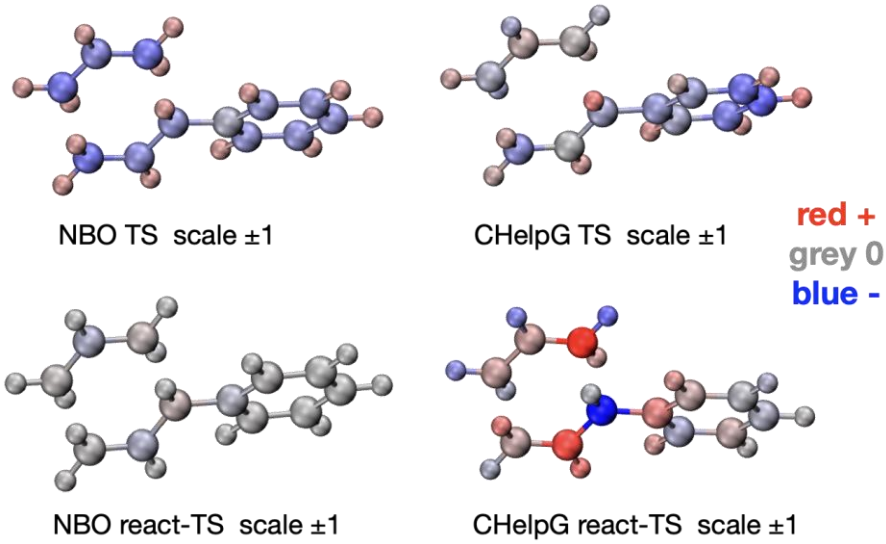

Figure S12.1 NBO and CHelpG charges for the gas-phase B3LYP-D3BJ/6-311+G(d,p) reactant and TS of reaction B, colour scale maxima are -1 (blue) through grey (0) to red (+1).

reactant				transition state				product			
no.	atm	ESP	NBO	no.	atm	ESP	NBO	no.	atm	ESP	NBO
1	C	-0.206	-0.381	1	C	0.086	-0.251	1	C	-0.076	-0.170
2	H	0.105	0.181	2	H	-0.110	0.194	2	H	0.093	0.189
3	H	-0.055	0.191	3	C	-0.057	-0.365	3	C	-0.596	-0.383
4	C	-0.077	-0.173	4	H	-0.133	0.197	4	H	0.135	0.181
5	H	0.185	0.198	5	C	0.033	-0.360	5	C	0.999	-0.410
6	C	-1.370	-0.401	6	H	-0.050	0.209	6	H	-0.324	0.210
7	H	-0.088	0.209	7	H	0.094	0.199	7	H	-0.069	0.194
8	H	0.383	0.205	8	H	0.139	0.205	8	H	0.082	0.191
9	C	3.328	-0.265	9	C	-0.006	-0.226	9	C	-0.535	-0.150
10	H	0.384	0.206	10	H	0.187	0.195	10	H	-0.213	0.193
11	C	-0.731	-0.156	11	C	-0.115	-0.204	11	C	-0.335	-0.208
12	H	-0.232	0.190	12	H	0.353	0.208	12	C	1.756	-0.424
13	C	-0.349	-0.375	13	C	-0.231	-0.368	13	H	-0.540	0.210
14	H	0.179	0.193	14	H	0.109	0.206	14	H	-0.575	0.211
15	H	-0.226	0.184	15	H	0.145	0.198	15	H	0.219	0.202
16	C	-0.508	-0.020	16	C	-0.167	-0.060	16	C	-0.052	-0.073
17	C	-0.252	-0.199	17	C	-0.137	-0.192	17	C	0.113	-0.197
18	C	0.003	-0.211	18	C	-0.100	-0.199	18	C	-0.227	-0.185
19	C	-0.362	-0.195	19	C	-0.380	-0.197	19	C	-0.523	-0.200
20	H	-0.125	0.205	20	H	0.111	0.202	20	H	0.416	0.206
21	C	-0.408	-0.195	21	C	-0.312	-0.195	21	C	-0.601	-0.201
22	H	0.002	0.202	22	H	0.226	0.202	22	H	0.377	0.205
23	C	-0.407	-0.211	23	C	-0.466	-0.213	23	C	-0.377	-0.207
24	H	0.305	0.206	24	H	0.231	0.205	24	H	0.130	0.205
25	H	0.206	0.205	25	H	0.228	0.205	25	H	0.282	0.206
26	H	0.315	0.206	26	H	0.323	0.206	26	H	0.441	0.205

Table S12.1 NBO and CHelpG charges for the B3LYP-D3BJ/6-311+G(d,p) gas-phase reactant, TS and product of reaction B.

no.	atm	ESP	NBO
1	C	0.16	-0.08
2	H	-0.30	0.00
3	C	0.15	0.02
4	H	-0.24	0.02
5	C	1.40	0.04
6	H	0.04	0.00
7	H	-0.29	-0.01
8	H	0.19	0.01
9	C	0.72	-0.07
10	H	0.42	0.00
11	C	-3.44	0.06
12	H	-0.03	0.00
13	C	0.12	0.01
14	H	-0.07	0.01
15	H	0.37	0.01
16	C	0.34	-0.04
17	C	0.11	0.01
18	C	-0.10	0.01
19	C	-0.02	0.00
20	H	0.24	0.00
21	C	0.10	0.00
22	H	0.22	0.00
23	C	-0.06	0.00
24	H	-0.07	0.00
25	H	0.02	0.00
26	H	0.01	0.00

Table S12.2 NBO and CHelpG charges for the B3LYP-D3BJ/6-311+G(d,p) gas-phase $q_{reactant}$ - q_{TS} of reaction B.

Section 13: Density Difference of TS-solvent clusters

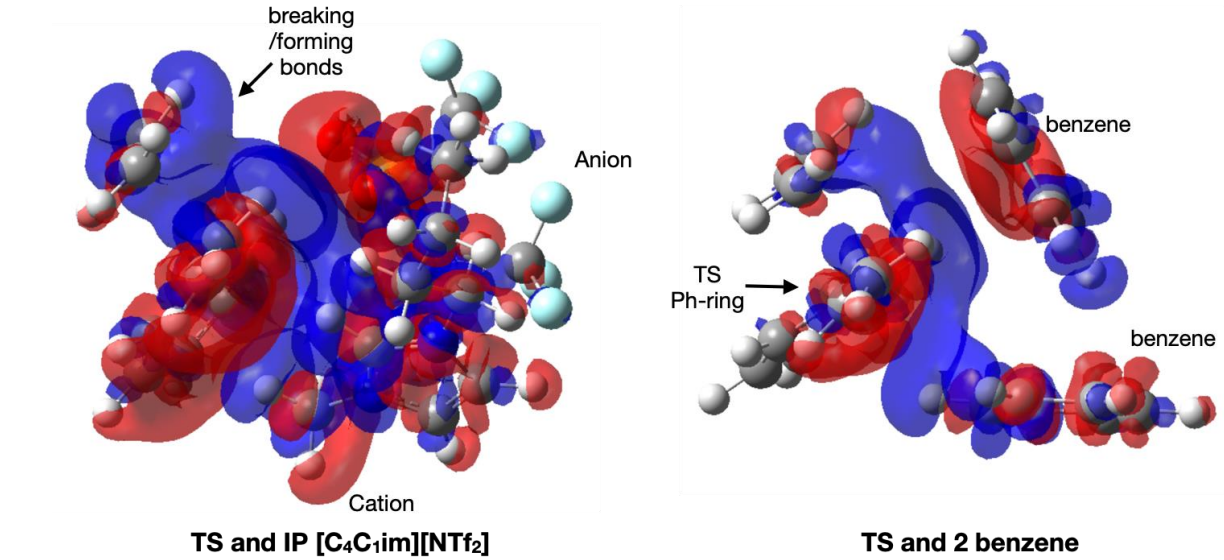

Figure S13.1 Density difference plots for the B3LYP-D3BJ/6-311+G(d,p) TS-solvent clusters evaluated in the gas-phase, mapped to the 0.0002au iso-density surface.

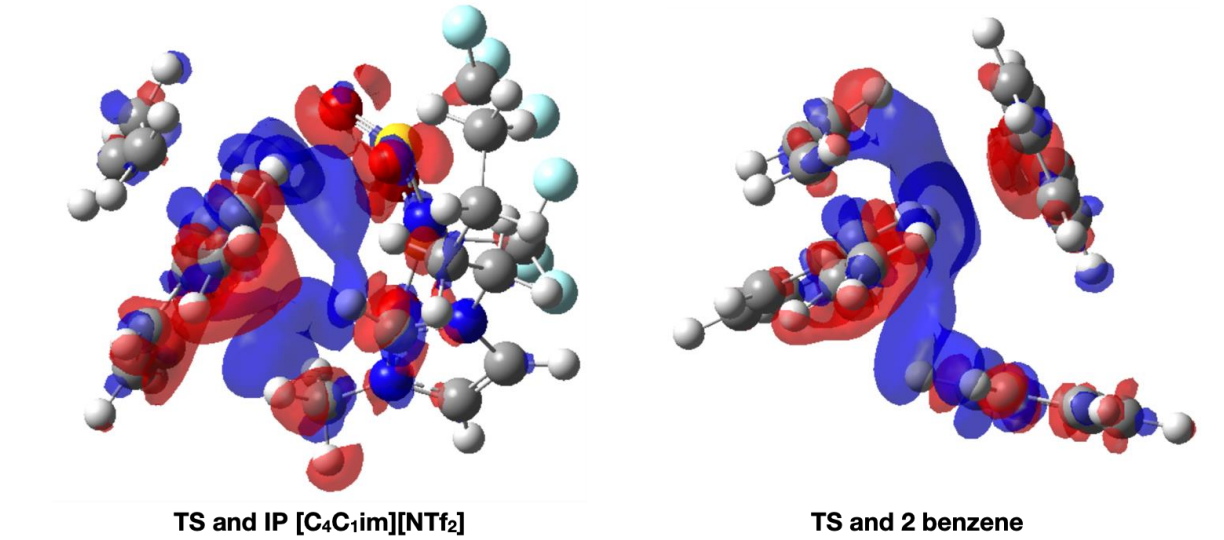

Figure S13.2 Density difference plots for the B3LYP-D3BJ/6-311+G(d,p) TS-solvent clusters evaluated with respective SMD generalised solvent environments, mapped to the 0.0002au iso-density surface.

Section 14: Comparing GP and SMD electrostatic polarisation

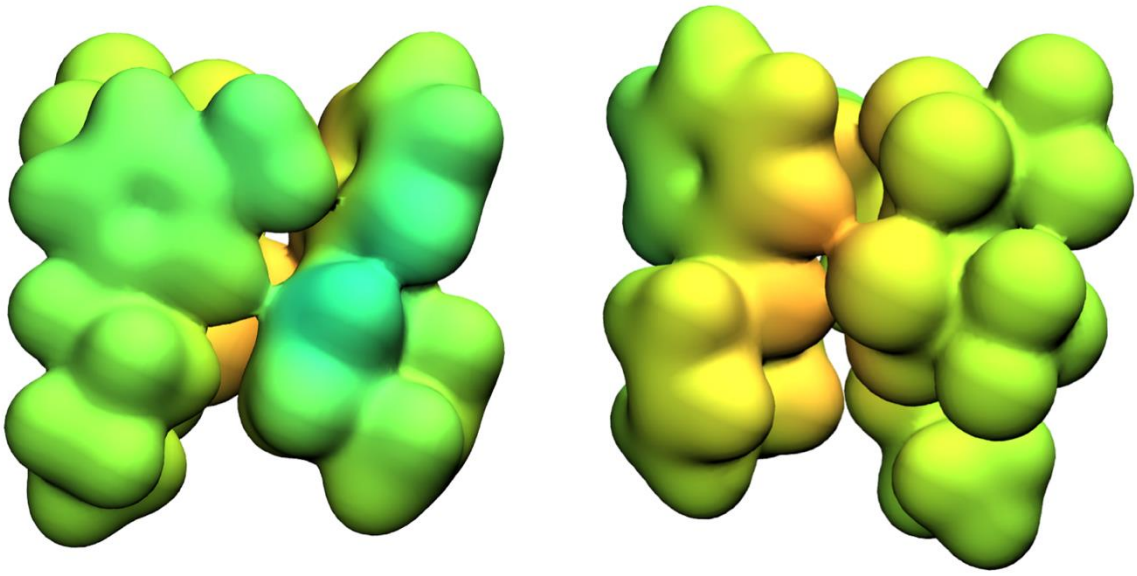

Figure S14.2 Reaction **B** TS-[$C_4C_1C_1$im][NTf_2] $\Delta ESP = ESP_{cluster} - (ESP_{TS} + ESP_{solvent})$ mapped onto the 0.007 au (e/a_0^3) density iso-surface. "Rainbow" colour scheme, blue=negative, green=neutral, red=positive, maximum ±0.02au.

.

Section 15: Computed Alpha

IL ion	α (a_0^3)
$[C_4C_1im]^+$	100
$[C_4C_1pyrr]^+$	106
$[C_4C_1C_1im]^+$	113
$[C_8C_1im]^+$	152
$[NTf_2]^-$	95
$[OTf]^-$	49

Table S15.1 Computed polarizability (α)of the ionic liquid ions, evaluate for B3LYP-D3(BJ)/6-311+G(d,p) optimised gas-phase structures.

Section 16: HPLC Data

HPLC calibration curve: Seven solutions of varying concentration of 1-phenyl-1,5-hexadiene in acetonitrile were prepared. A stock solution of naphthalene standard in acetonitrile was prepared (0.01 mmol/ml). 0.5 ml (0.005 mmol) of naphthalene standard was added to each of the prepared 1-phenyl-1,5-hexadiene solutions. The mixtures were analysed by HPLC and the ratio between product and standard signal was used to generate a calibration curve to quantify the product formation in reaction B.

Calibration	Volume [ml]	n(Product) [mmol]	A(Standard)	A(Product)	Ratio
1	1.5	0.00735	593154	11789519	19.88
2	1	0.00490	798026	10415217	13.05
3	0.5	0.00245	1446191	8521449	5.89
4	0.4	0.00196	1442483	6828108	4.73
5	0.3	0.00147	1432381	5163903	3.61
6	0.2	0.00098	1421133	3443107	2.42
7	0.1	0.00049	1424167	1677122	1.18

Table S14.1 Calibration data

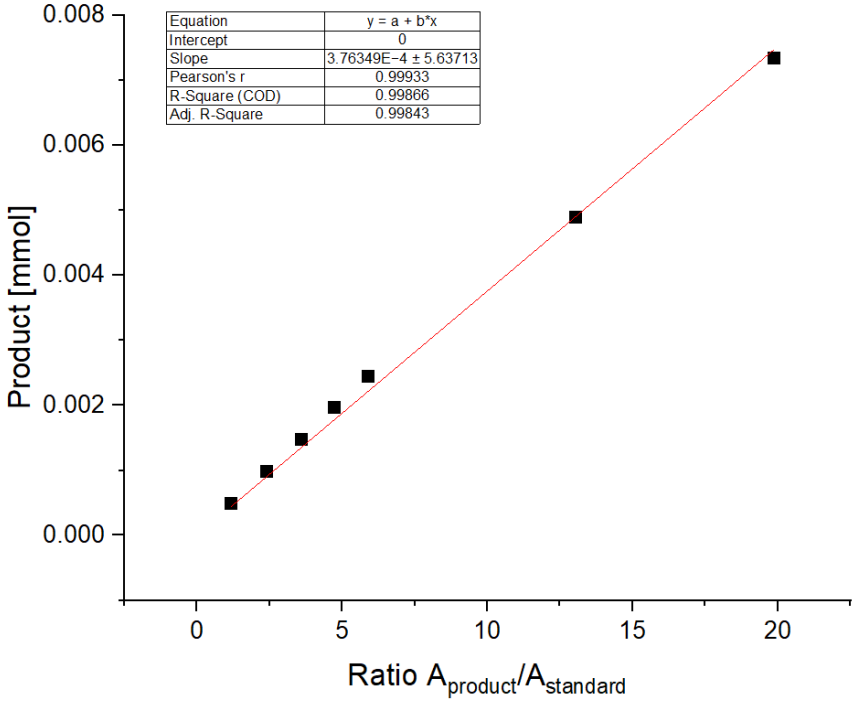

Figure S14.1 Calibration curve used to quantify the product of reaction B.

General procedure for reaction B

A solution of 3-phenyl-1,5-hexadiene in the relevant solvent was prepared, for exact quantities see Table **S13.1** (approx. 0.021 mmol/ml). The solution was then transferred to a pressure tube and sealed. The reaction was run at 150^{o}C for 17h. Upon completion the reaction was cooled to RT to stop further rearrangement. For non-viscous samples, a sample (0.6ml) was taken and mixed with the standard. For viscous samples, taking accurate aliquots was not feasible and in these cases the reaction mixture was directly mixed with the standard in the pressure tube. The solution of reaction mixture and standard was diluted with acetonitrile and analysed by HPLC.

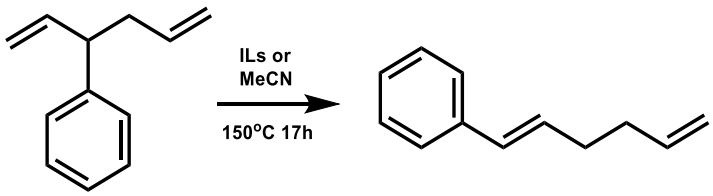

Figure S14.2 Conditions for screening of solvent for Reaction B.

Solvent	Run	Conc. reaction [mmol/ml]	Volume solvent [ml]	Sample taken [ml]	Sample amount [mmol]
MeCN	A	0.0211	3	0.6	0.0126
	B	0.0211	3	0.6	0.0126
[C_4C_1im] [NTf_2]	A	0.0209	1.2	whole sample	0.0251
	B	0.0209	1.1	whole sample	0.0230
[$C_4C_1C_1$im][NTf2]	A	0.0216	1.1	whole sample	0.0238
	B	0.0216	1.1	whole sample	0.0237
[C_4C_1pyrr][NTf2]	A	0.0212	1.2	whole sample	0.0254
	B	0.0212	1.2	whole sample	0.0254
[C_4C_1im][OTf]	A	0.0202	1.2	whole sample	0.0242
	B	0.0202	1.2	whole sample	0.0242
[C_8C_1im][OTf]	A	0.0211	1.2	whole sample	0.0254
	B	0.0211	1.2	whole sample	0.0254

Table S14.2: Reaction setup for reaction B.

Solvent	Run	Sample amount [mmol]	A (standard)	A (product)	Ratio	n(product)	conversion %
MeCN	A	0.0126	349534	600714	1.72	0.0006	**5.12**
	B	0.0126	348396	497851	1.43	0.0005	**4.26**
$[C_4C_1im]$ $[NTF_2]$	A	0.0251	327400	3818131	11.66	0.0044	**17.50**
	B	0.0230	346548	3822888	11.03	0.0042	**18.06**
$[C_4C_1C_1im][NTf_2]$	A	0.0238	336051	3516358	10.46	0.0039	**16.58**
	B	0.0237	324136	3554685	10.97	0.0041	**17.38**
$[C_4C_1pyrr][NTF_2]$	A	0.0254	259036	2597177	10.03	0.0038	**14.87**
	B	0.0254	303296	2781154	9.17	0.0035	**13.60**
$[C_4C_1im][OTf]$	A	0.0242	336494	3293733	9.79	0.0037	**15.22**
	B	0.0242	323997	3052039	9.42	0.0035	**14.64**
$[C_8C_1im][NTf_2]$	A	0.0254	322064	2692611	8.36	0.0031	**12.40**
	B	0.0254	323997	3052039	9.42	0.0035	**13.97**

Table S14.3 HPLC data and quantified conversion [%] for reaction B.

Section 17: NMR of Relevant Compounds

$[C_4C_1im][NTf_2]$

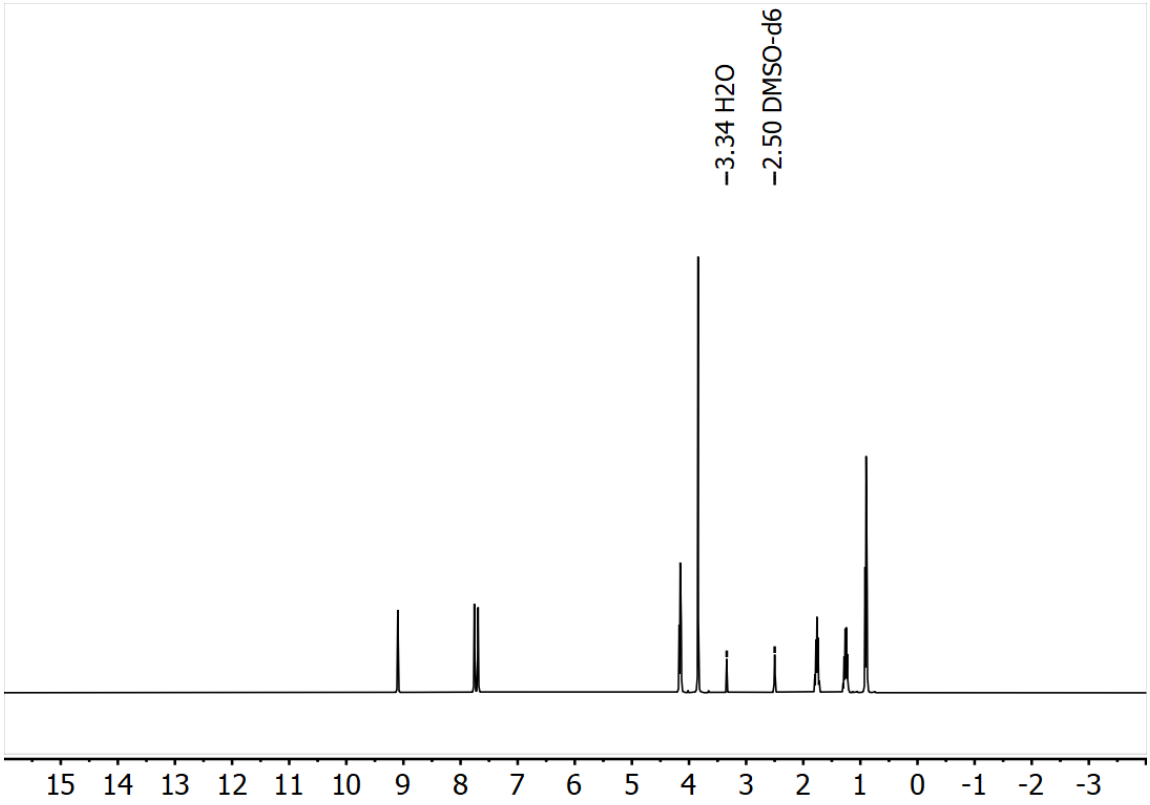

Figure S15.1: ^{1}H spectra of $[C_4C_1im][NTf_2]$ in DMSO-d_6.

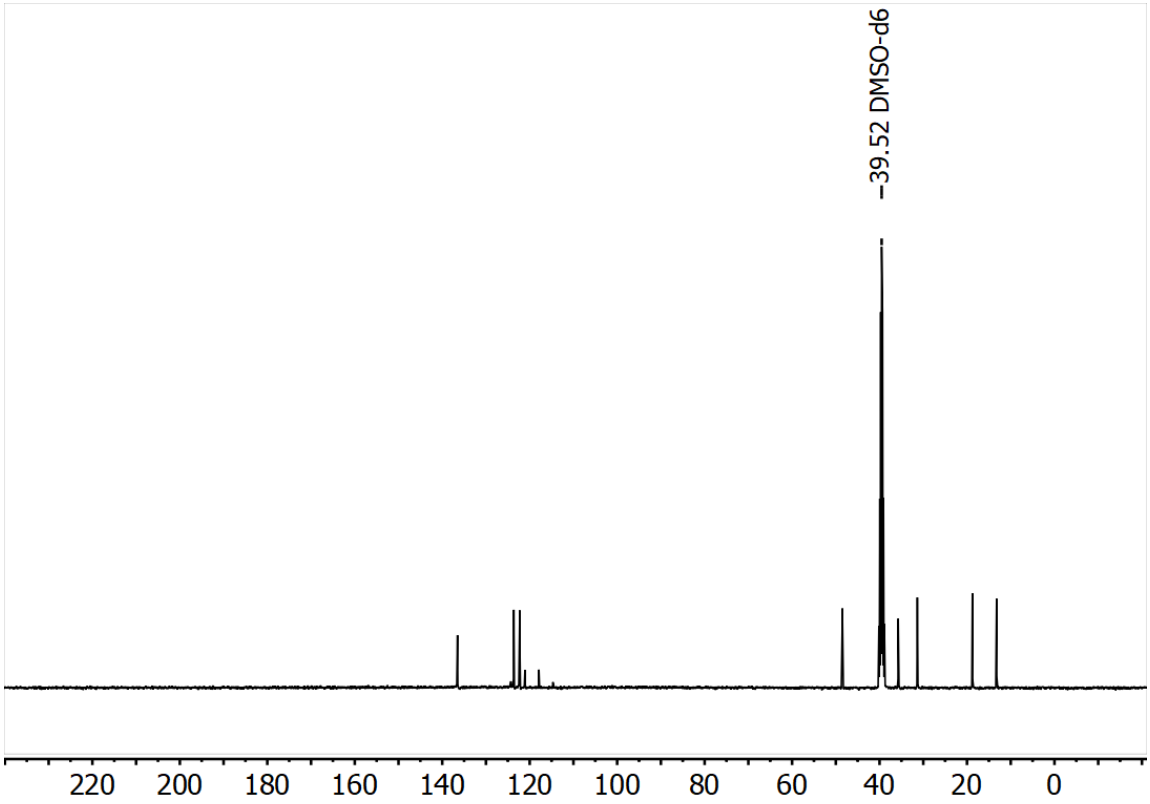

Figure S15.2: $^{13}C\{^{1}H\}$ spectra of $[C_4C_1im][NTf_2]$ in DMSO-d_6.

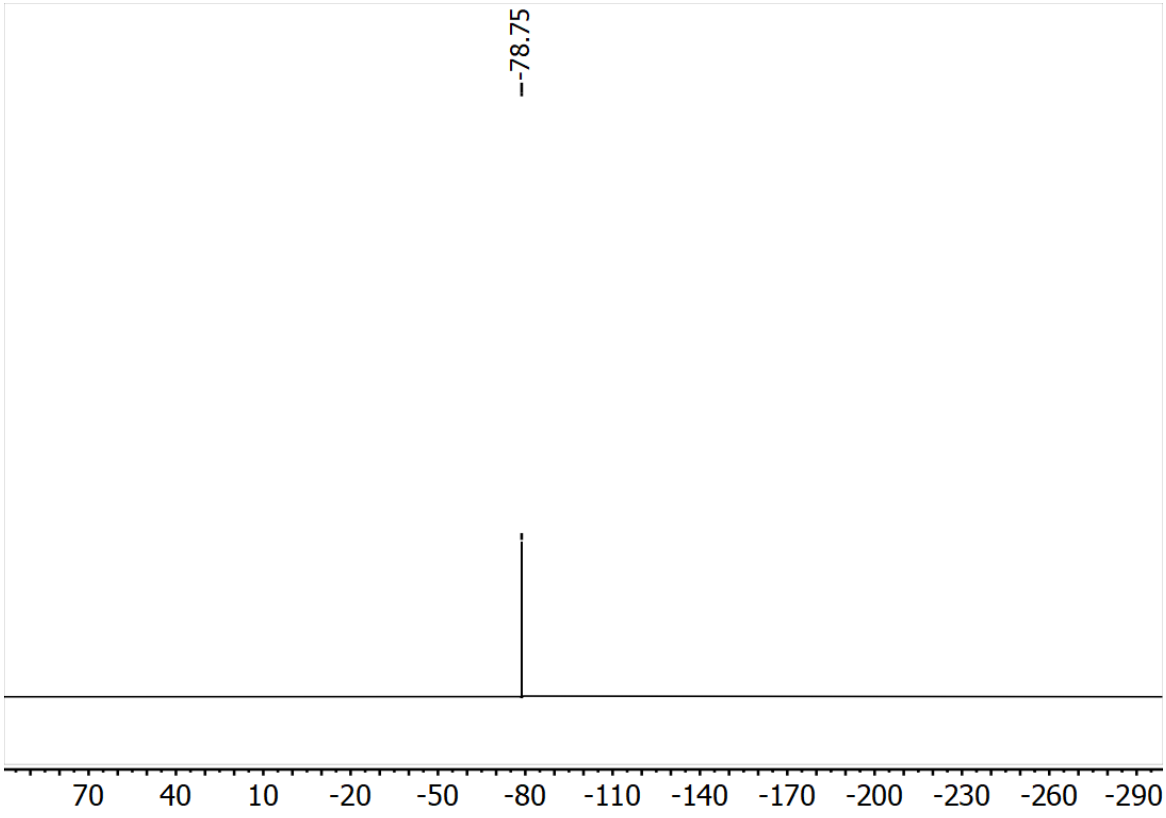

Figure S15.3: ^{19}F spectra of $[C_4C_1im][NTf_2]$ in DMSO-d_6.

$[C_4C_1im][OTf]$

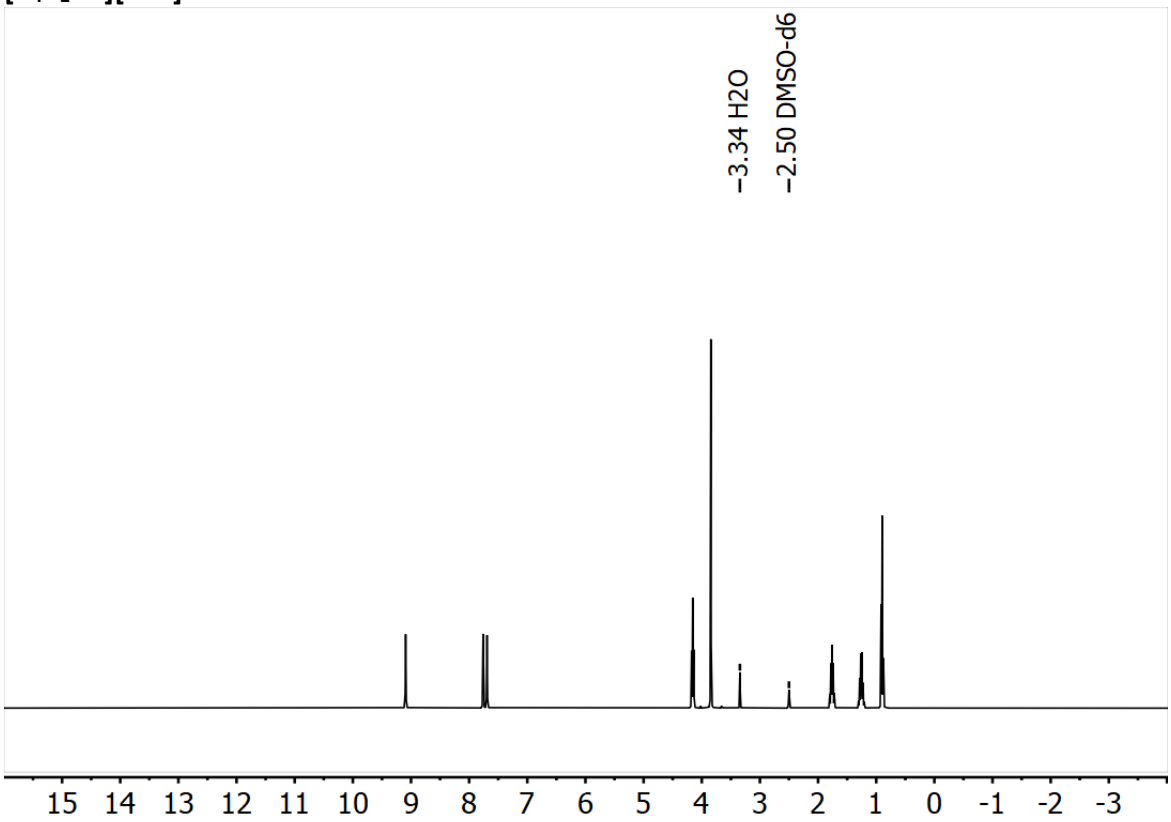

Figure S15.4: ^{1}H spectra of $[C_4C_1im][OTf]$ in DMSO-d_6.

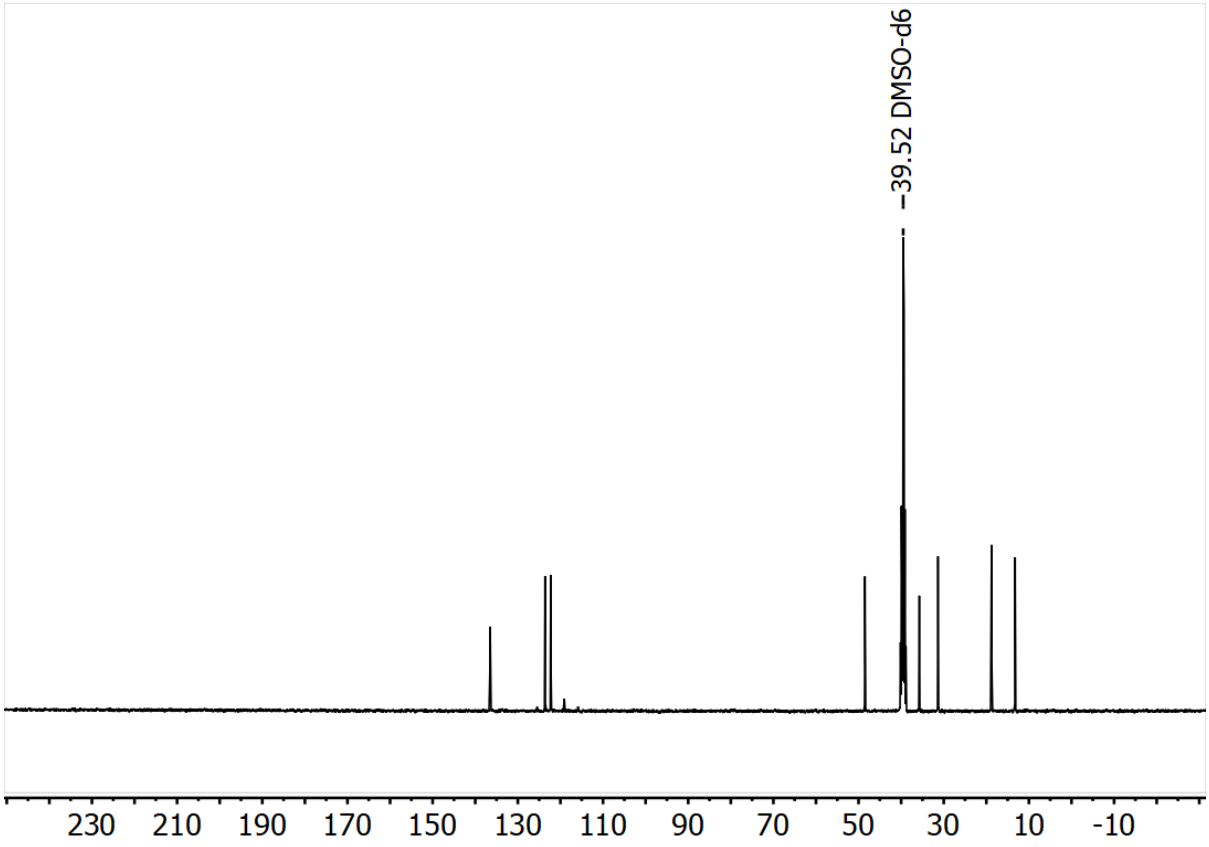

Figure S15.5: $^{13}C\{^{1}H\}$ spectra of $[C_4C_1im][OTf]$ in DMSO-d_6.

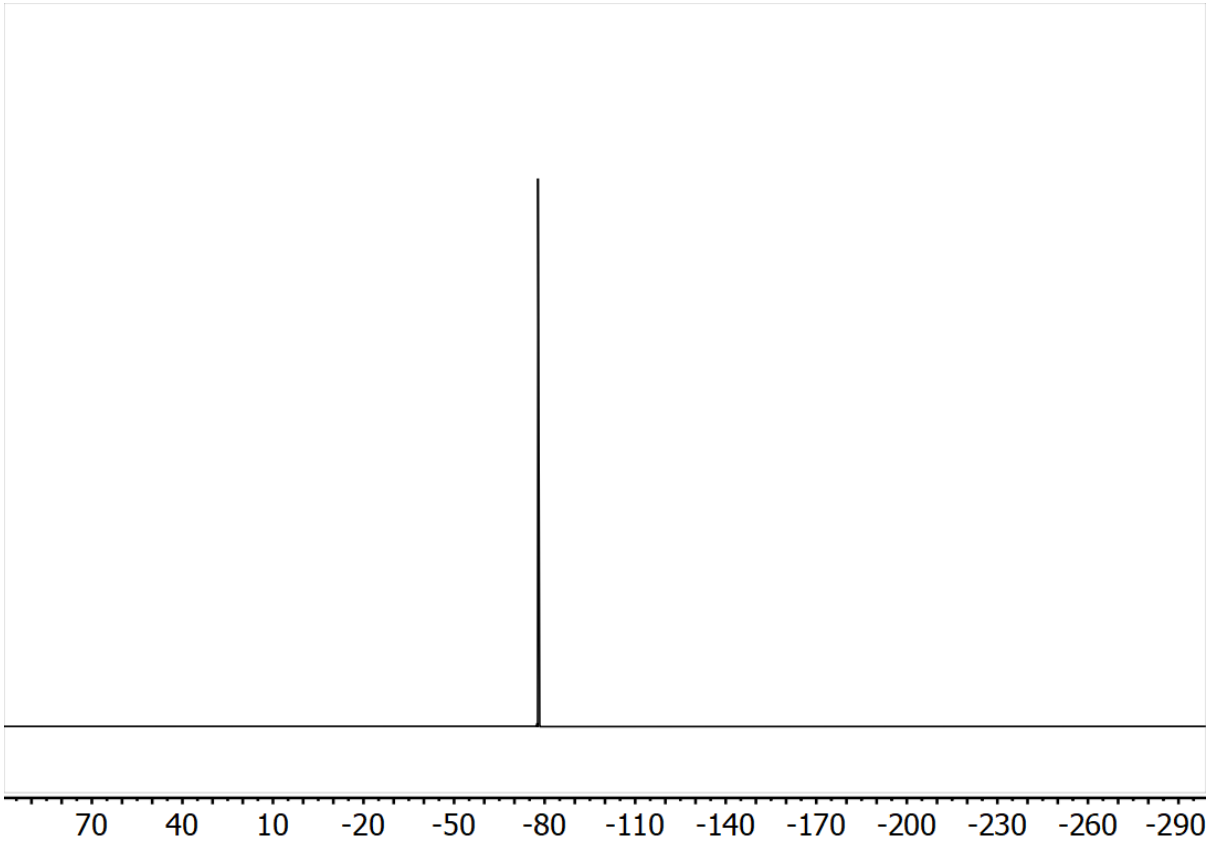

Figure S15.6: ^{19}F spectra of $[C_4C_1im][OTf]$ in DMSO-d_6.

[$C_4C_1C_1$im][NTf_2]

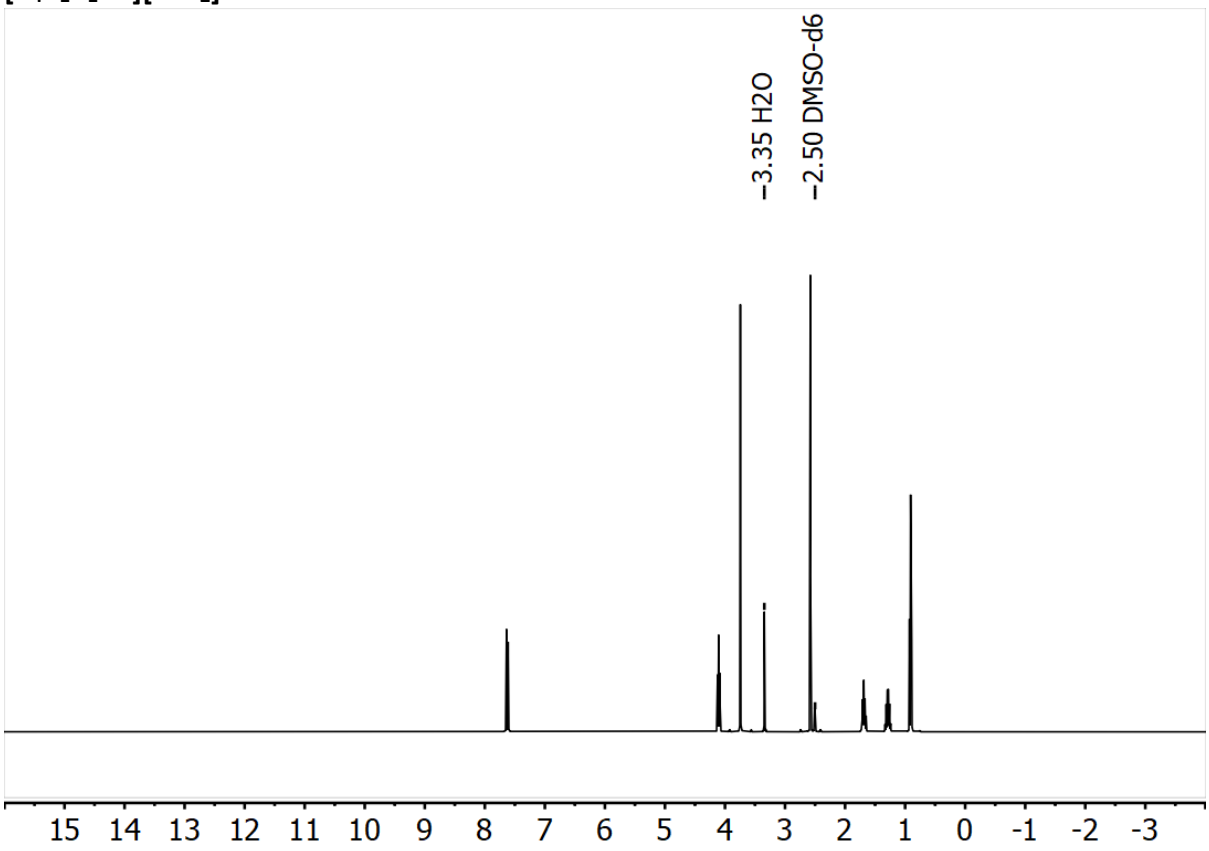

Figure S15.7: ^{1}H spectra of [$C_4C_1C_1$im][NTf_2] in DMSO-d_6.

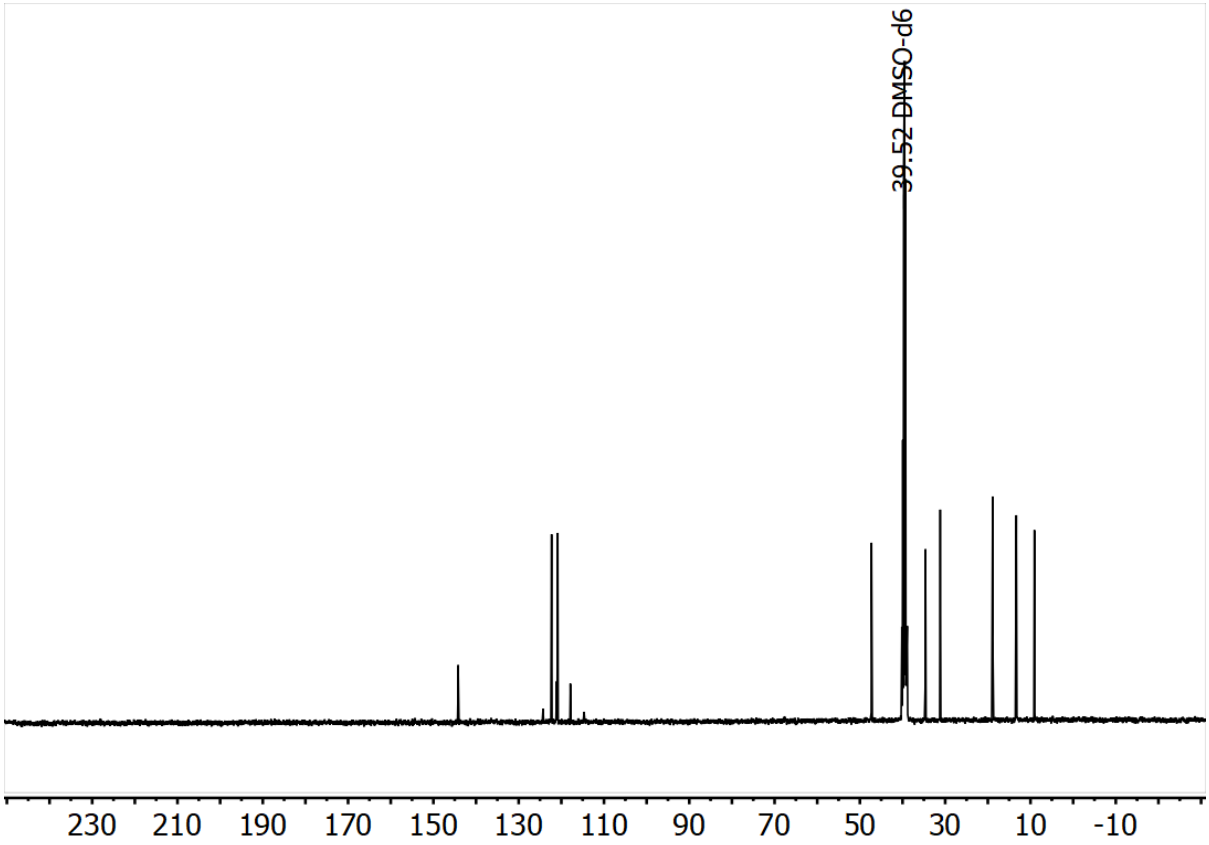

Figure S15.8: $^{13}C\{^{1}H\}$ spectra of [$C_4C_1C_1$im][NTf_2] in DMSO-d_6.

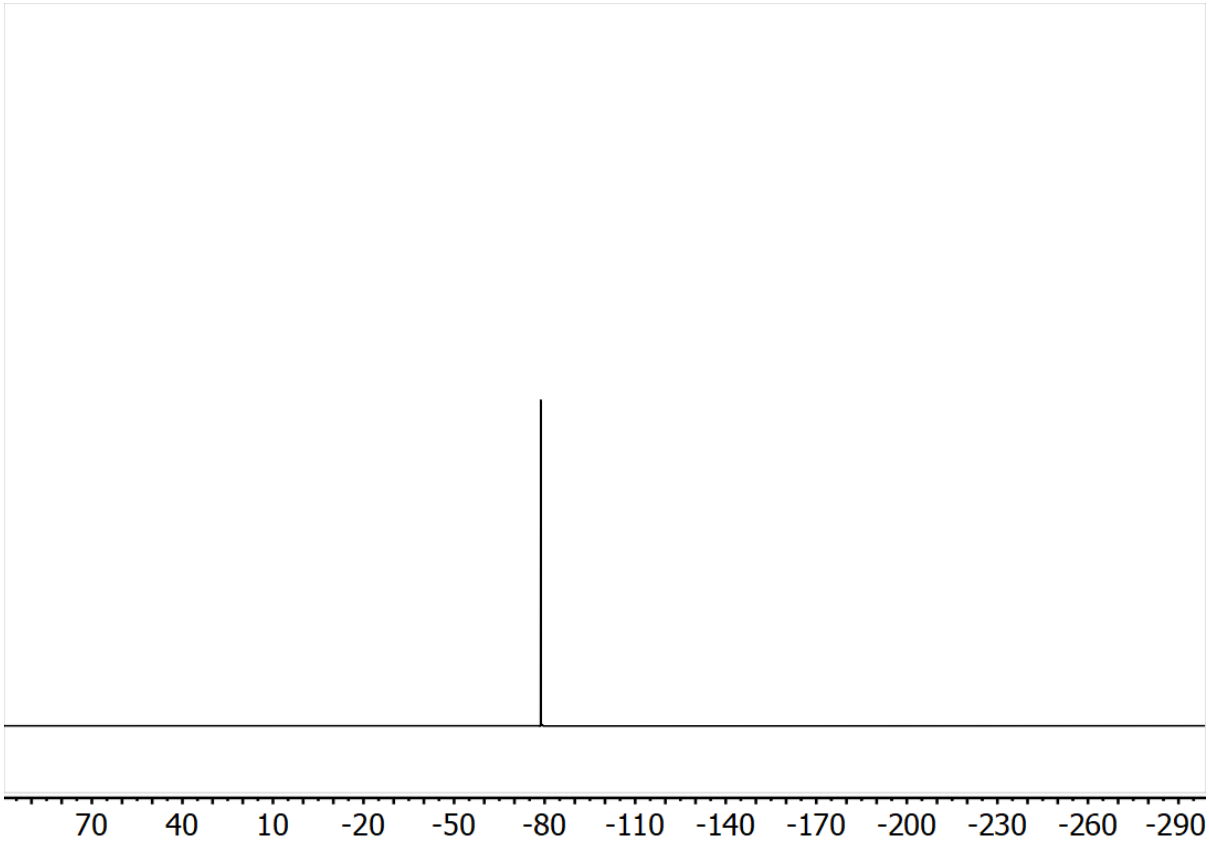

Figure S15.9: ^{19}F spectra of $[C_4C_1C_1im][NTf_2]$ in DMSO-d_6.

$[C_4C_1pyrr][NTf_2]$

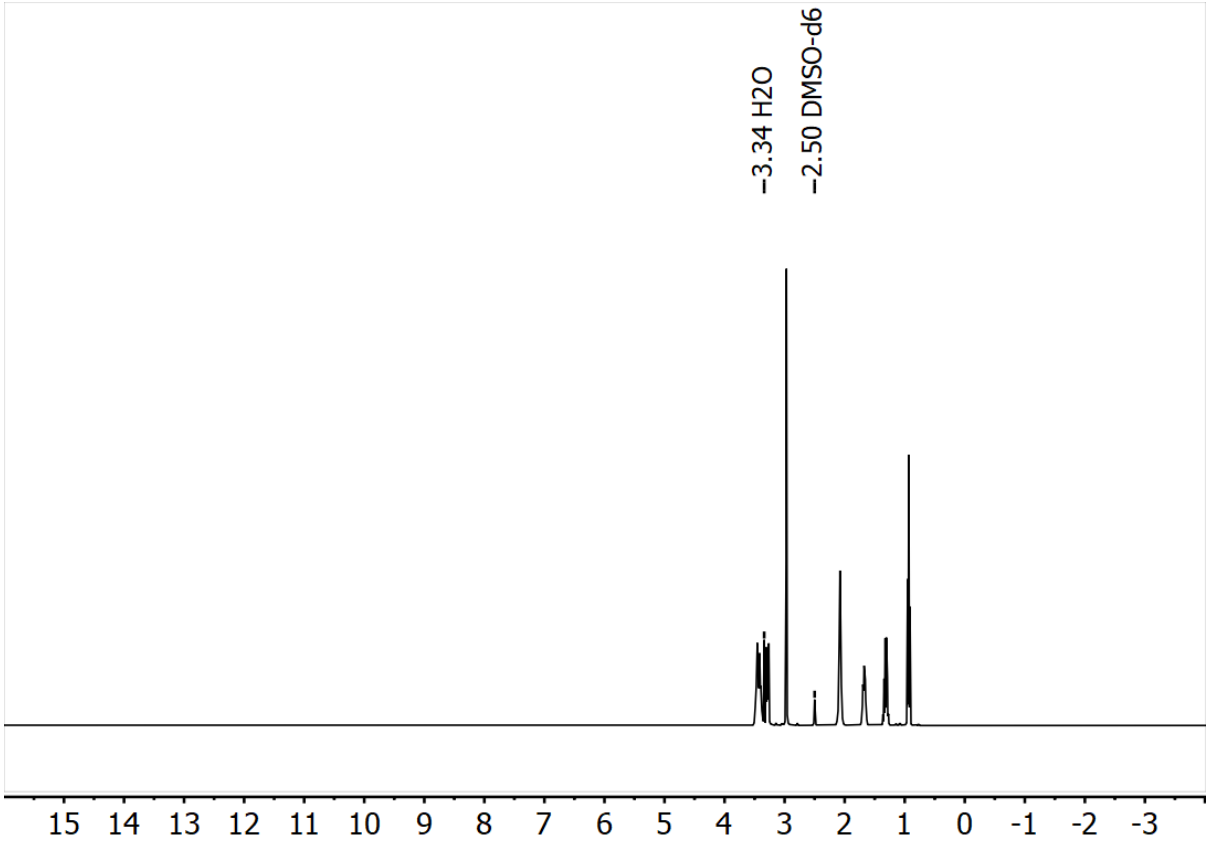

Figure S15.10: ^{1}H spectra of $[C_4C_1pyrr][NTf_2]$ in DMSO-d_6.

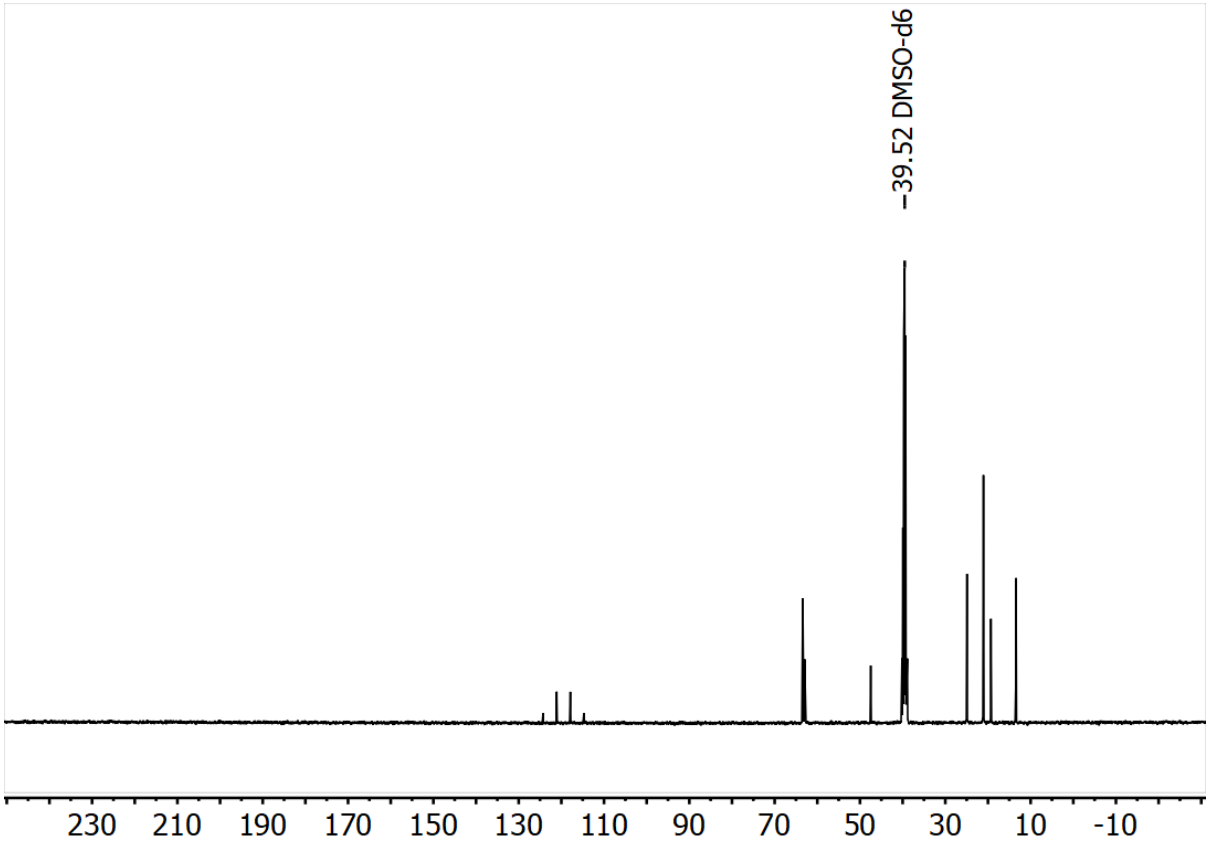

Figure S15.11: $^{13}C\{^{1}H\}$ spectra of $[C_4C_1pyrr][NTf_2]$ in DMSO-d_6.

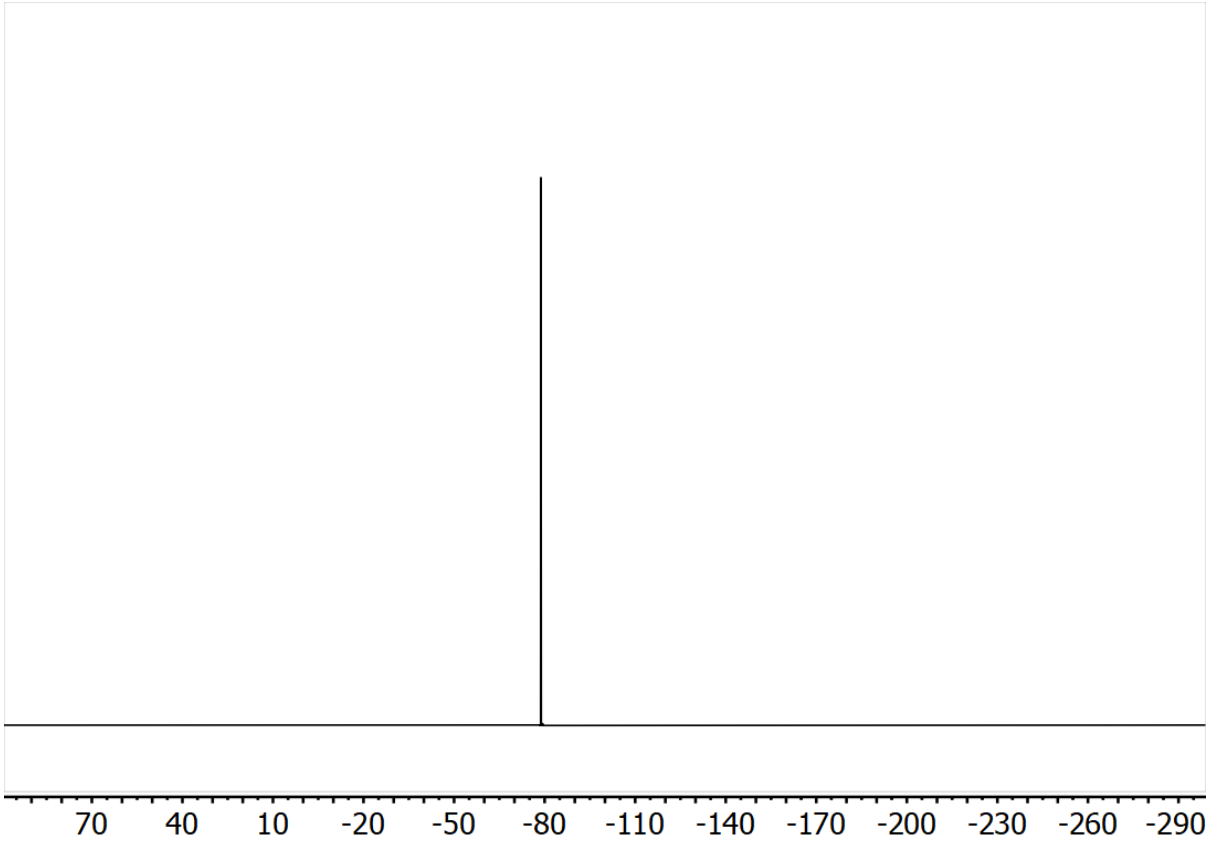

Figure 15.12: ^{19}F spectra of $[C_4C_1pyrr][NTf_2]$ in DMSO-d_6.

3-Phenyl-1,5-hexadiene

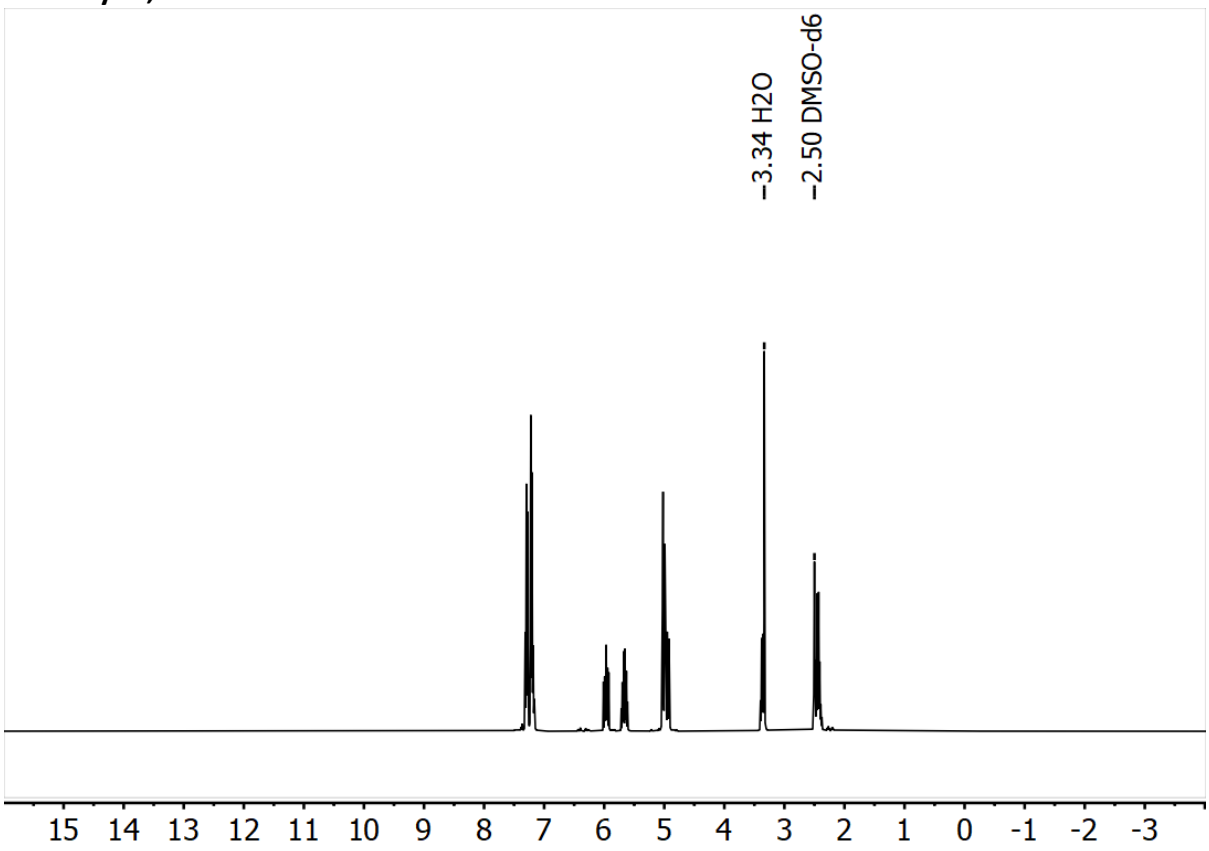

Figure 15.13: ^{1}H spectrum of 3-phenyl-1,5-hexadiene in DMSO-d_6.

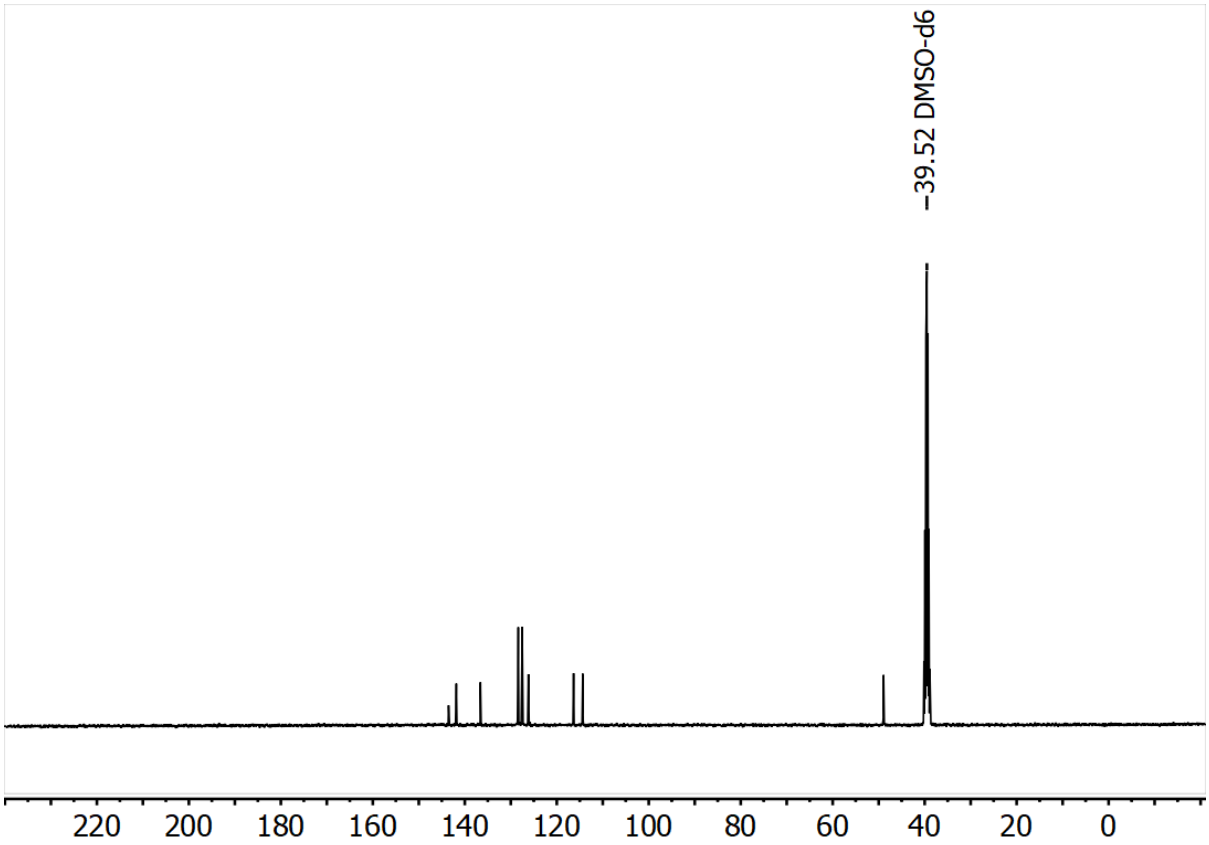

Figure 15.14: $^{13}C\{^{1}H\}$ spectrum of 3-phenyl-1,5-hexadiene in DMSO-d_6.

1-Phenyl-1,5-hexadiene

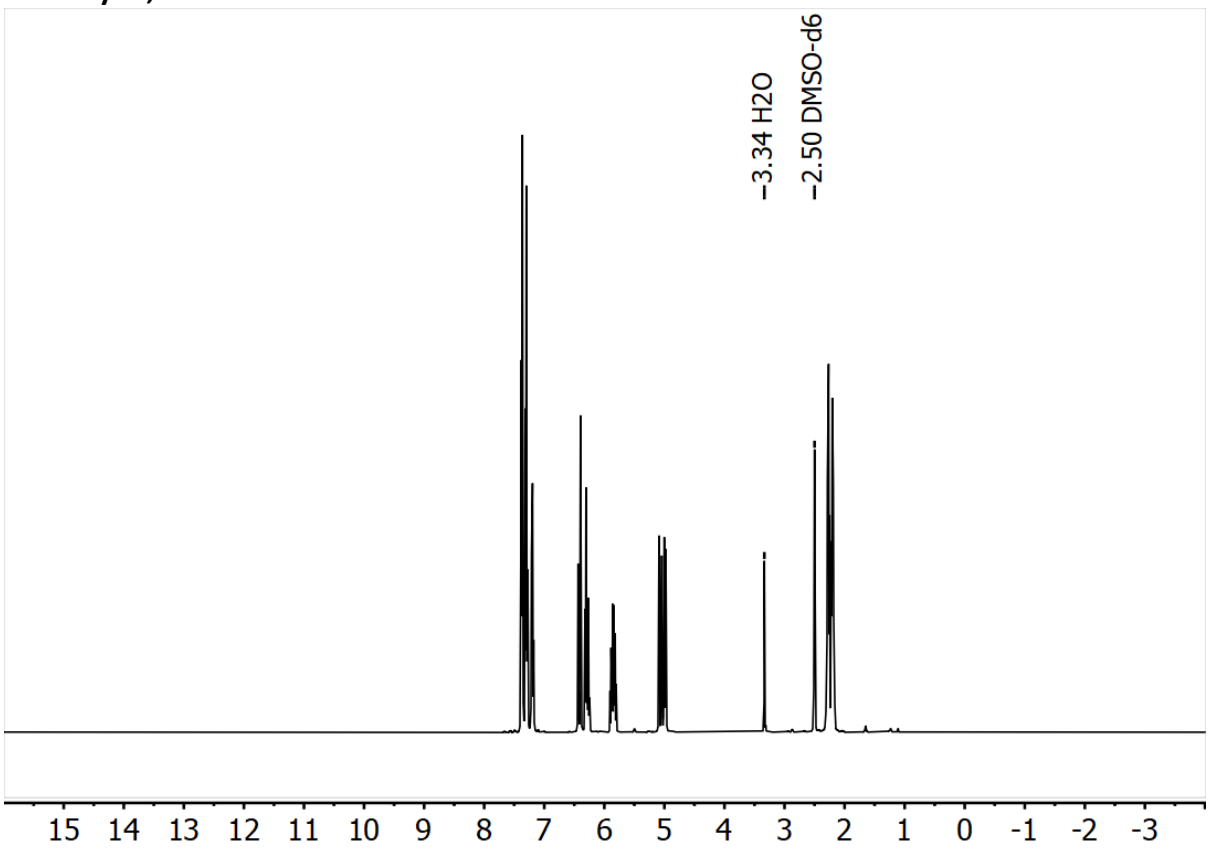

Figure 2: ^{1}H spectra of 1-phenyl-1,5-hexadiene in DMSO-d_6.

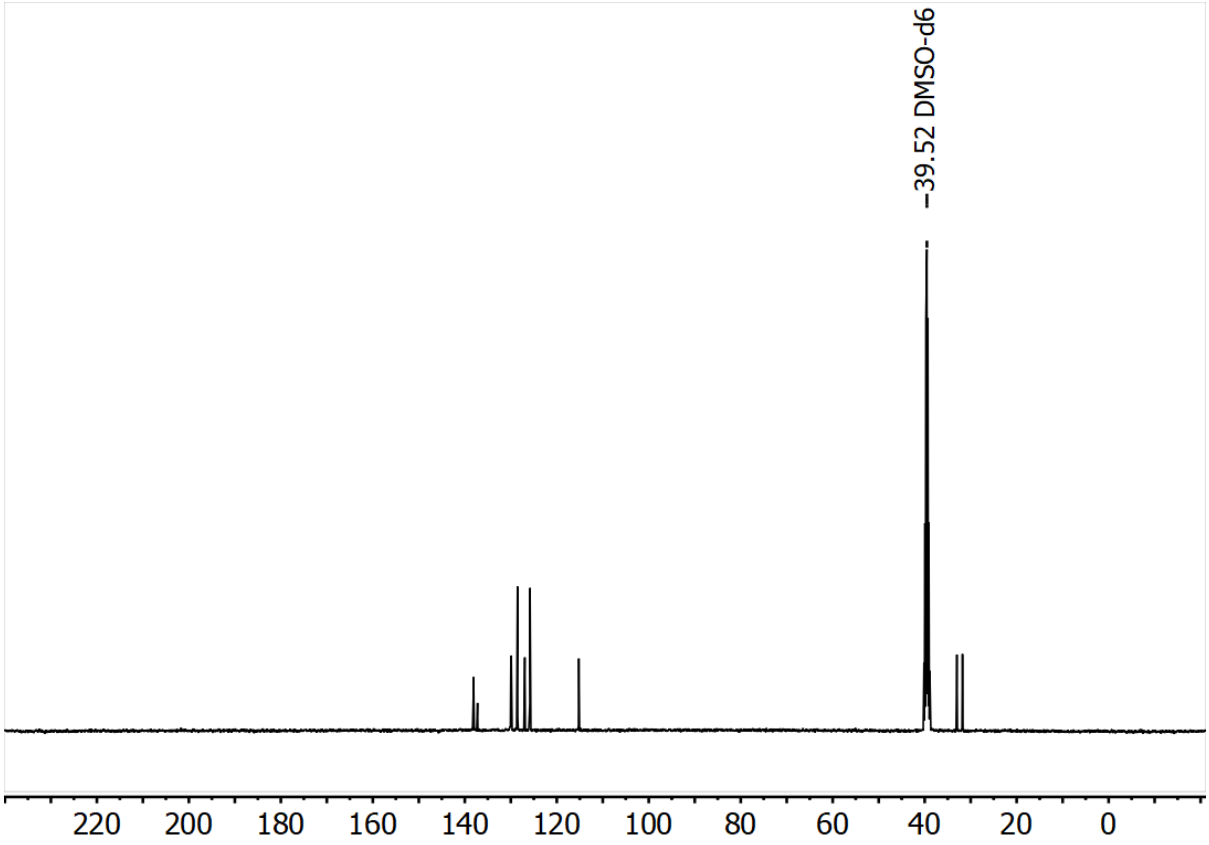

Figure 15.16: $^{13}C\{^{1}H\}$ spectra of 3-phenyl-1,5-hexadiene in DMSO-d_6.